Echocardiography for Cardiac Resynchronization Therapy: Recommendations for Performance and Reporting–A Report from the American Society of Echocardiography Dyssynchrony Writing Group *Endorsed by the Heart Rhythm Society*

John Gorcsan III, MD, Theodore Abraham, MD, Deborah A. Agler, RDMS, Jeroen J. Bax, MD, Genevieve Derumeaux, MD, Richard A. Grimm, DO, Randy Martin, MD, Jonathan S. Steinberg, MD, Martin St. John Sutton, MD, and Cheuk-Man Yu, MD,
Pittsburgh and Philadelphia, Pennsylvania; Baltimore, Maryland; Cleveland, Ohio; Leiden, The Netherlands; Lyon, France; Atlanta, Georgia; New York, New York; Hong Kong, China

Echocardiography plays an evolving and important role in the care of heart failure patients treated with biventricular pacing, or cardiac resynchronization therapy (CRT). Numerous recent published reports have utilized echocardiographic techniques to potentially aide in patient selection for CRT prior to implantation and to optimized device settings afterwards. However, no ideal approach has yet been found. This consensus report evaluates the contemporary applications of echocardiography for CRT including relative strengths and technical limitations of several techniques and proposes guidelines regarding current and possible future clinical applications. Principal methods advised to qualify abnormalities in regional ventricular activation, known as dyssynchrony, include longitudinal velocities by color-coded tissue Doppler and the difference in left ventricular to right ventricular ejection using routine pulsed Doppler, or interventricular mechanical delay. Supplemental measures of radial dynamics which may be of additive value include septal-to-posterior wall delay using M-mode in patients with non-ischemic disease with technically high quality data, or using speckle tracking radial strain. A simplified post-CRT screening for atrioventricular optimization using Doppler mitral inflow velocities is also proposed. Since this is rapidly changing field with new information being added frequently, future modification and refinements in approach are anticipated to continue.

Keywords: Echocardiography, Doppler ultrasound, Congestive Heart Failure, Pacing Therapy

Echocardiography plays an important role in the care of patients with heart failure treated with cardiac resynchronization therapy (CRT). A large number of clinical reports have utilized echocardiography before CRT implantation to assess abnormalities of mechanical activation, known as dyssynchrony, to potentially improve patient selection or guide lead placement. In addition, echocardiography has been advocated to optimize the CRT device settings afterward. The purpose of this consensus report is to evaluate the contemporary state-of-the-art applications of echocardiography for CRT and to propose guidelines regarding current and potential future clinical applications. We acknowledge that this is a relatively young and rapidly changing field with new information being discovered continually. Because no optimal approach has yet been clearly defined, the strengths and limitations of the principal current techniques will be discussed along with practical recommendations.

From the University of Pittsburgh, Pittsburgh, Pennsylvania (J.G.), Johns Hopkins University, Baltimore, Maryland (T.A.), Cleveland Clinic, Cleveland, Ohio (D.A.A., R.A.G.), University of Leiden, Leiden, The Netherlands (J.J.B.), Université Clude Bernard, Lyon, France (G.D.), Emory University, Atlanta, Georgia (R.M.), St. Luke's-Roosevelt Hospital, New York, New York (J.S.S.), University of Pennsylvania, Philadelphia, Pennsylvania (M.St.J.S.), and The Chinese University of Hong Kong, Hong Kong, China (C-M.Y.).

Theodore Abraham, MD received research grants from GE Ultrasound. Jeroen Bax, MD received research grants from GE, BMS, Guidant, Medtronic, and St. Jude. Richard Grimm, DO is on the Speaker Bureau and a Consultant on the Advisory Board of Medtronic. John Gorcsan, MD received research grants from Toshiba, GE, and Siemens; and is also a Consultant on the Advisory Board of Toshiba, GE, and Siemens. Jonathan Steinberg, MD received research grants from Medtronic, St. Jude, and Boston Scientific; and he is also a Consultant on the Advisory Board of Boston Scientific. Cheuk-Man Yu, MD received research grants from GE, Medtronic, and Pfizer; and is also on the Speaker Bureau of Medtronic and GE and a Consultant on the Advisory Board of Medtronic, Boston Scientific, and GE.

Reprint requests: John Gorcsan III, MD, University of Pittsburgh, Scaife Hall 564, 200 Lothrop St, Pittsburgh, PA 15213-2582 (E-mail: gorcsanj@upmc.edu).

0894-7317/$34.00

doi:10.1016/j.echo.2008.01.003

CLINICAL BENEFITS OF RESYNCHRONIZATION THERAPY

CRT has had a major favorable impact on the care of patients with heart failure, left ventricular (LV) systolic dysfunction, and mechanical dyssynchrony, routinely identified by electrocardiography (ECG) as abnormal electrical activation. CRT, also referred to as biventricular pacing, has been shown in several randomized clinical trials to improve heart failure functional class, exercise capacity, and quality of life, in addition to reducing hospitalizations and prolonging survival[1-7]

Table 1 Summary of important clinical trials of cardiac resynchronization therapy

	MUSTIC	PATH-CHF	MIRACLE	MIRACLE-ICD
Inclusion criteria	NYHA III LVEF < 35% EDD > 60 mm 6-min walk < 450 m QRS ≥ 150 ms	NYHA III, IV QRS ≥ 120 ms	NYHA III, IV LVEF ≤ 35% EDD ≥ 55 mm QRS ≥ 130 ms	NYHA III, IV LVEF ≤ 35% EDD ≥ 55 mm QRS ≥ 130 ms ICD indication
Sample	58	40	453	369
End points	QOL, 6-min walk, peak VO_2, HF hospitalization	Acute hemodynamics QOL, 6-min walk, HF hospitalization	QOL, NYHA class, 6-min walk, composite	QOL, NYHA class, 6-min walk
Study design	Single-blind, randomized, crossover	Single-blind, randomized, crossover	Double-blind, randomized, parallel-controlled	Double-blind, randomized, parallel-controlled
Treatment arms	CRT vs no pacing	CRT vs no pacing	CRT vs no pacing	CRT-D vs ICD
Major findings	CRT improved all end points, reduced hospitalization	CRT improved acute hemodynamics and chronic end points	CRT improved all end points; reduced HF hospitalization	CRT improved QOL and NYHA class only, and did not impair ICD function

	CONTAK	COMPANION	CARE-HF
Inclusion criteria	NYHA II-IV LVEF ≤ 35% QRS ≥ 120 ms ICD indication	NYHA III, IV LVEF ≤ 35% QRS ≥ 120 ms	NYHA III, IV LVEF ≤ 35% QRS > 150 ms or QRS = 120-150 with dyssynchrony
Sample	333	1520	819
End points	Composite of mortality, HF hospitalization and VT/VF	Primary: all-cause mortality or hospitalization; secondary: all-cause mortality	All-cause mortality or unplanned hospitalization
Study design	Double-blind, randomized, parallel-controlled	Randomized, parallel-controlled	Randomized, parallel-controlled
Treatment arms	CRT-D vs ICD	CRT vs CRT-D vs no pacing	CRT vs no pacing
Major findings	CRT improved secondary end points; primary end points did not improve	CRT and CRT-D improved primary end point; CRT-D; reduced mortality	CRT improved primary end point and reduced all cause mortality

CRT, Cardiac resynchronization therapy; *CRT-D*, cardiac resynchronization therapy-defibrillator; *EDD*, left ventricular end-diastolic diameter; *HF*, heart failure, *ICD*, implantable cardioverter defibrillator; *LVEF*, left ventricular ejection fraction; *NYHA*, New York Heart Association; *QOL*, quality of life score, *VF*, ventricular fibrillation; *VO_2*, maximal oxygen consumption; *VT*, ventricular tachycardia.

(Table 1). Furthermore, CRT is associated with reductions in mitral regurgitation (MR) and improvements in LV function.[2,8-12] Currently approved recommendations for CRT include patients with severe heart failure: New York Heart Association (NYHA) functional class III or IV, widened QRS greater than or equal to 120 milliseconds, and LV ejection fraction (EF) less than or equal to 35%.[13] Despite the great success of randomized clinical trails, approximately 25% to 35% of patients undergoing CRT do not respond favorably. Echocardiographic and Doppler imaging techniques have emerged to play a potential role in the care of the patient with CRT. Although there are several potential reasons for nonresponse to CRT, it has been suggested that the ECG widened QRS is a suboptimal marker for dyssynchrony, and that echocardiographic quantification of dyssynchrony may potentially play a role in improving patient selection for CRT.[12,14-16] The PROSPECT study (predictors of responders to CRT) was a recent observational multicenter study from Europe, the United States, and Hong Kong.[17,18] Although final data from this study are not yet available, the preliminary findings highlighted the complexity of technical factors that influence dyssynchrony analyses and the importance of training and expertise of individual laboratories to achieve reliable results. The PROSPECT study suggested that there are technical issues related to variability that are not yet resolved, and that future work is needed to improve reproducibility of dyssynchrony analysis.

OVERVIEW OF MECHANICAL DYSSYNCHRONY

Electrical activation in the normal heart typically occurs quickly within 40 milliseconds via conduction through the Purkinje network and is associated with synchronous regional mechanical contraction. A variety of myocardial diseases induce alterations in cardiac structure and function that result in regions of early and late contraction, known as dyssynchrony.[19] Although other authors have used the term "asynchrony" interchangeably, we will use the term "dyssyn-

chrony" in this report to describe this phenomenon. Mechanical dyssynchrony is usually associated with a prolonged QRS duration on the surface ECG, although it may also exist in a subset of patients with heart failure and depressed LV function and narrow QRS by ECG.[20,21] This report will focus on patients with wide QRS duration, because this is the current clinical practice for CRT.

Three types of cardiac dyssynchrony may occur: intraventricular, interventricular, and atrioventricular (AV). Abnormalities of timing of regional mechanical LV activation, known as intraventricular dyssynchrony, appear to be the principal factor associated with contractile impairment and affected by CRT. Accordingly, many echocardiographic Doppler parameters focus on intraventricular dyssynchrony, and we will use the term "dyssynchrony" throughout this report when referring to "intraventricular dyssynchrony," unless otherwise stated. The classic type of dyssynchrony resulting from abnormal electrical activation is seen with left bundle branch block. The typical pattern seen with left bundle branch block is early activation of the interventricular septum and late activation of the posterior and lateral LV walls.[19] The early septal contraction occurs before normal ejection when LV pressure is low and does not contribute to ejection. This process generates heterogeneous stress and strain in the LV, with one wall exerting forces on the contralateral wall. Typically early septal contraction causes posterior-lateral stretching or thinning, followed by late posterior-lateral contraction causing septal stretching or thinning.[22] Dyssynchrony results in inefficient LV systolic performance, increases in end-systolic volume and wall stress, and delayed relaxation that is thought to affect biological signaling processes involved in regulating perfusion and gene expression.[23] Improvements in LV synchrony are associated with LV functional improvements and reduction in MR.[8,24-28]

GENERAL APPROACH TO QUANTIFYING MECHANICAL DYSSYNCHRONY

Because the vast majority of patients with wide QRS appear to have mechanical dyssynchrony, an important goal of imaging is to improve patient selection for CRT by identifying the subset of patients with wide QRS but no mechanical dyssynchrony. The pathophysiologic reason for this scenario is unclear, but it appears that patients with minimal to no dyssynchrony have a lower probability of response to CRT and appear to have a poor prognosis after CRT.[15] There are other reasons for not responding to CRT, including ischemic disease with too much scar to reverse remodel, subsequent infarction after CRT, suboptimal lead placement, and other factors not yet defined.[24,29-33] Accordingly, the absence of dyssynchrony is only one factor for nonresponse, but one that potentially can be identified prospectively by echocardiographic Doppler methods.

Results from the PROSPECT study illustrated that technical factors of individual echocardiographic Doppler methods, such as feasibility and reproducibility, affect results in a multicenter setting.[17,18] Quantifying mechanical dyssynchrony in a series of patients with heart failure is complex, and no single ideal method currently exists. However, a practical approach that considers several factors is currently recommended to assist in determining that a patient has or does not have significant dyssynchrony. Ambiguities that may occur in analysis using different approaches must be adjudicated on a case-by-case basis. A reasonable starting point is to examine the routine 2-dimensional (2D) echocardiographic images. Trained observers can often assess dyssynchrony visually as an early septal in-and-out motion described as septal flash or bounce in typical left bundle branch block dyssynchrony. Because the presence or absence of dyssynchrony may be subtle in many patients with severe heart failure, visual assessment should not stand alone and the use of quantitative echocardiographic Doppler tools is advocated.

M-MODE

The technically simplest approach to quantify LV dyssynchrony is with conventional M-mode echocardiography that records septal-to-posterior wall-motion delay (Figure 1, *A*).

Step 1: Select either the parasternal long-axis or short-axis views.

Step 2: Position the M-mode cursor at the midventricular level (papillary muscle level).

Step 3: Set sweep speed to 50 to 100 mm/s.

Step 4: Identify the time delay from peak inward septal motion to peak inward posterior wall.

Pitzalis et al reported a cut-off value of greater than or equal to 130 milliseconds as a marker of LV dyssynchrony in a pilot series of 20 patients principally with nonischemic cardiomyopathy with a sensitivity of 100% and specificity of 63% to predict a greater than or equal to 15% decrease in LV end- systolic volume index, and improvements in clinical outcome.[34,35] Longer delays in septal to posterior wall-motion delay were associated with greater reverse remodeling. Measurement of the septal-to-posterior wall-motion delay by M-mode may be difficult in many patients because of complex septal motion that is both active and passive–wall-motion abnormalities involving the septum or posterior wall. Marcus et al highlighted these limitations in an analysis of M-mode data from 79 patients in the CONTAK-CD trial.[36] They found the reproducibility of M-mode measurements to be unsatisfactory, with responders (defined as ≥15% reduction in LV end-systolic volume) having septal-to-posterior wall-motion delays similar to nonresponders. The PROSPECT study also identified a high degree of variability in analysis.[17,18] Therefore, M-mode is not advocated to be used in isolation to quantify dyssynchrony, but may be considered as supplemental to other approaches, such as tissue Doppler (TD). In particular, the utility of M-mode in patients with ischemic cardiomyopathy has not been well demonstrated.

COLOR TD M-MODE

The addition of color TD M-mode is a useful adjunct to M-mode determination of LV dyssynchrony (Figure 1, *B*). Changes in direction are color coded, which may aid in identifying the transition from inward to outward motion in the septum and posterior wall. The same septal-to-posterior wall-motion delay greater than or equal to 130 milliseconds is considered to be significant dyssynchrony, although this method is affected by similar limitations with routine M-mode as described above.

LONGITUDINAL TD VELOCITY

The largest body of literature to quantify dyssynchrony is represented by the assessment of longitudinal LV shortening velocities using TD from the apical windows.[14-16,37-49] This is the principal method currently in clinical use, although it has limitations discussed subsequently. There are two basic approaches: color-coded or pulsed TD.

COLOR TD DATA ACQUISITION

Color TD data acquisition is simpler and more practical than pulsed TD and is the preferred method by consensus of this committee if

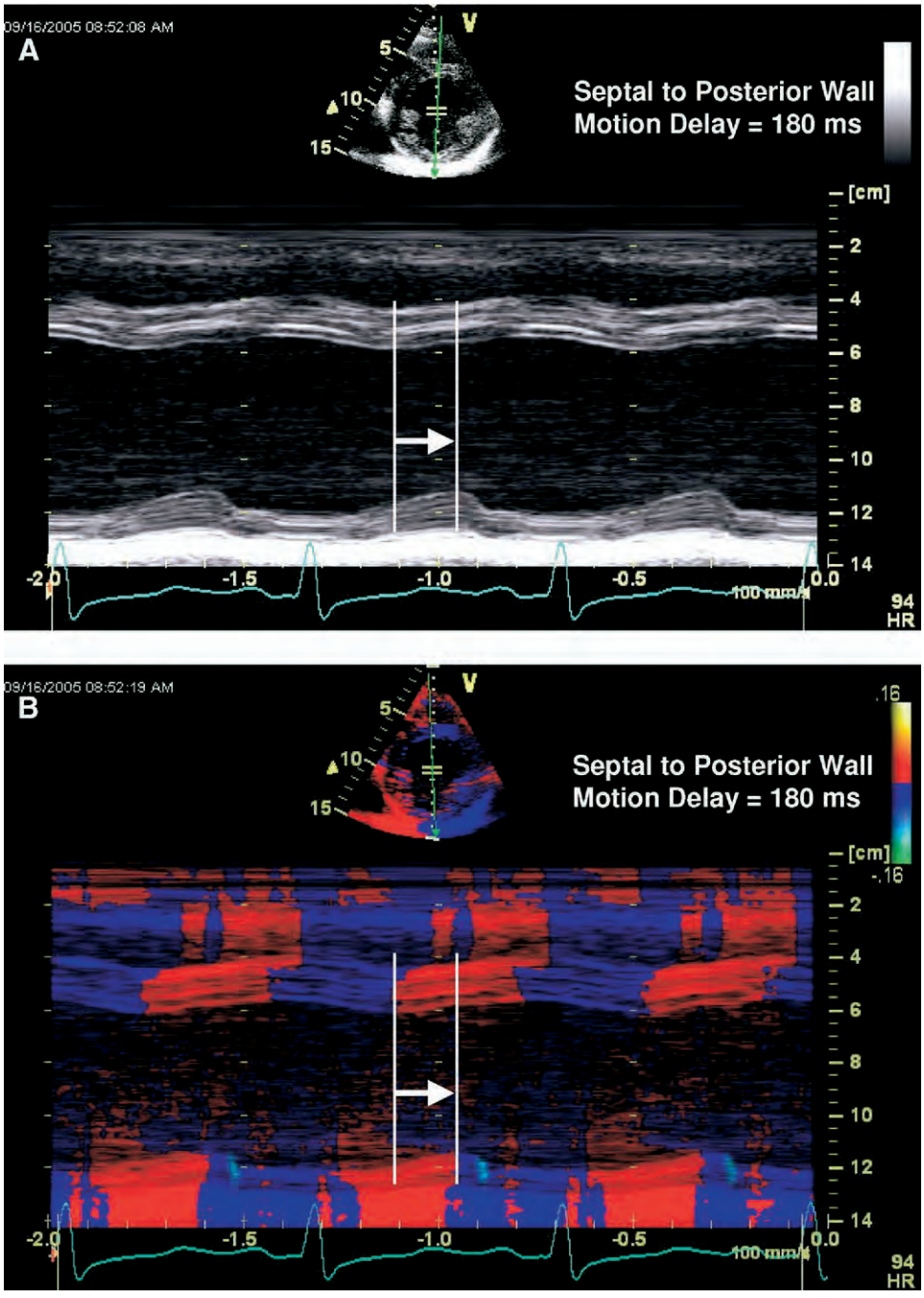

Figure 1 Routine M-mode (**A**) at midventricular level and color-coded tissue Doppler M-mode (**B**) demonstrating septal to posterior wall delay of 180 milliseconds, consistent with significant dyssynchrony (≥130 milliseconds).

high frame rate color TD echocardiographic equipment is available. High frame–rate color TD, usually greater than 90 frames/s, is available in several major equipment vendors with recent hardware and software. Individual variations in color TD between ultrasound systems may exist, but these details have not yet been elucidated.

Step 1: Adjust the ECG to be noise free with a delineated QRS waveform.

Step 2: Optimize 2D imaging to insure maximal apical-to-near field left atrial imaging, with overall gain and time gain control settings adjusted for clear myocardial definition.

Step 3: Position the LV cavity in the center of the sector and aligned as vertically as possible, to allow for the optimal Doppler angle of incidence with LV longitudinal motion.

Step 4: Set the depth to include the level of the mitral annulus.

Step 5: Activate color TD and adjust the sector to include the entire LV with a goal of achieving high frame rates (usually >90 frames/s). Decrease depth and sector width to focus on the LV to increase frame rates, as needed. Adjust overall color gain for clear delineation of the myocardium. If available, the online color coding of time to peak velocity data may be activated.

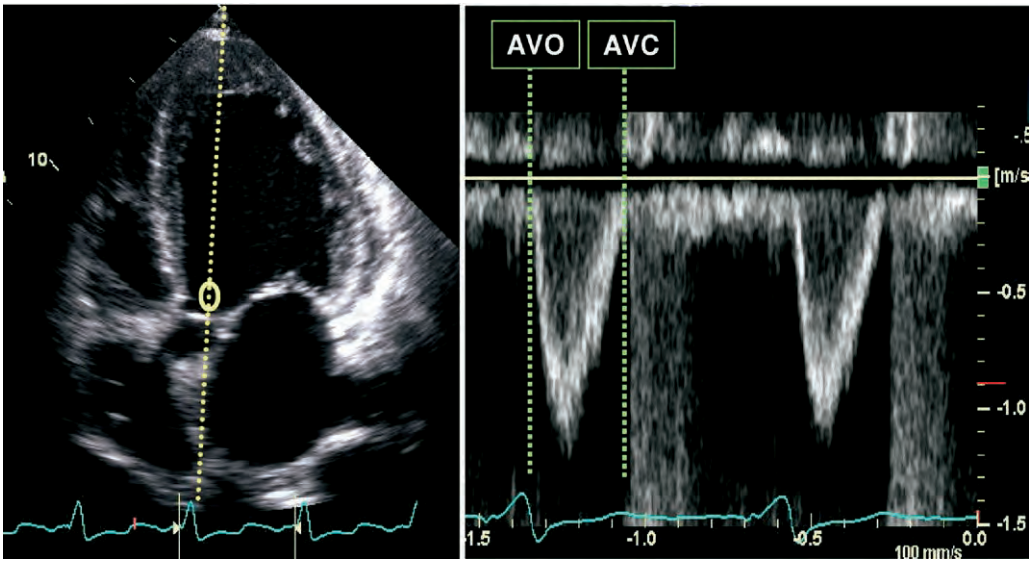

Figure 2 Determination of left ventricular ejection interval from pulsed Doppler of outflow tract. *AVC*, Aortic valve closure; *AVO*, aortic valve opening.

Step 6: Suspend patient breathing. Because low velocity TD data are affected by respiratory motion, we recommend that patients be instructed to hold their breath transiently if they are able, while a 3- to 5-beat digital capture is performed. This is usually at end expiration, but may be the phase with the optimal image quality. The number of beats captured should be increased if atrial or ventricular premature complexes are present.

Step 7: Record 3 standard imaging planes: apical 4-chamber view, apical 2-chamber view, and apical long-axis view.

Step 8: Determine the LV ejection interval. This is usually done using pulsed Doppler from an apical 5-chamber or apical long-axis view where the LV outflow tract is seen and velocity recorded (Figure 2).

COLOR TD DATA ANALYSIS

A major advantage of color DTI is the ability to analyze time-velocity data offline. The details for analysis vary by ultrasound vendor, but the general steps are similar.

Step 1: Determine the timing of LV ejection, usually from the beginning to the end of pulsed Doppler flow of the LV outflow tract. The details vary according to ultrasound system used, but timing usually is performed using the ECG as a time marker. The timing of beginning ejection to end ejection is then superimposed as the ejection interval on the subsequent time-velocity curve analysis.

Step 2: Size and place regions of interest (a minimum of 5 × 10 mm to 7 × 15 mm) in the basal and midregion of opposing LV walls (4 regions/view) to determine time-velocity plots.

Step 3: If possible, identify components of velocity curve, as a check for physiologic signal quality. These include isovolumic contraction velocity (usually <60 milliseconds from the onset of the QRS), the systolic wave, or S wave, moving toward the transducer and the early diastolic, or E wave, and late diastolic, or A wave, moving away from the transducer (Figures 3 and 4).

Step 4: Manually adjust the regions of interest within the segment both longitudinally and side-to-side within the LV wall to identify the site where the peak velocity during ejection is most reproducible. This is an important step to search for the most reproducible peak of greatest height, in particular where there is more than one peak or signal noise. If fine tuning of the region of interest fails to produce a single reproducible peak during ejection, the earlier peak is chosen if there are two or more peaks of the same height.

Step 5: Determine time from onset of the QRS complex to the peak systolic velocity for each region: 4 segments per view, for each of 3 views, for a total of 12 segments. An alternative is to determine the difference in the time to peak S wave from opposing walls, as described in the opposing wall delay method below. This is simply the time from the S wave of one wall to the S wave of the opposing wall on the same cineloops, and does not require measuring the onset from the QRS.

Step 6: Average the time to peak values in captured beats to improve reproducibility, because beat-to-beat variability may occur. A minimum of averaging 3 to 5 beats is recommended, with the number of averaged beats increased if beat-to-beat variability is encountered, excluding sequences with atrial or ventricular premature complexes. Analysis of TD data in atrial fibrillation is especially complex and problematic, and no data are currently available to support dyssynchrony analysis in this scenario.

POSTSYSTOLIC SHORTENING VELOCITIES

Some previous studies have included postsystolic shortening (positive myocardial velocity after aortic valve closure, which may be greater than the ejection peak) in their dyssynchrony analysis.[47] The greatest sensitivity and specificity for predicting response to CRT appears to be attained when limiting peak longitudinal velocities for dyssynchrony analysis to the interval from aortic valve opening to aortic valve closure.[37,43] Notabartolo et al[47] measured the maximal difference in the time to peak systolic velocity including postsystolic shortening from the 6 basal segments. An average cut-off value greater than 110 milliseconds has a high sensitivity at 97%, but decreased specificity at 55% to predict LV reverse remodeling. Although the optimal approach has not yet been completely clarified, the current weight of evidence favors analysis of peak velocities during the ejection interval.

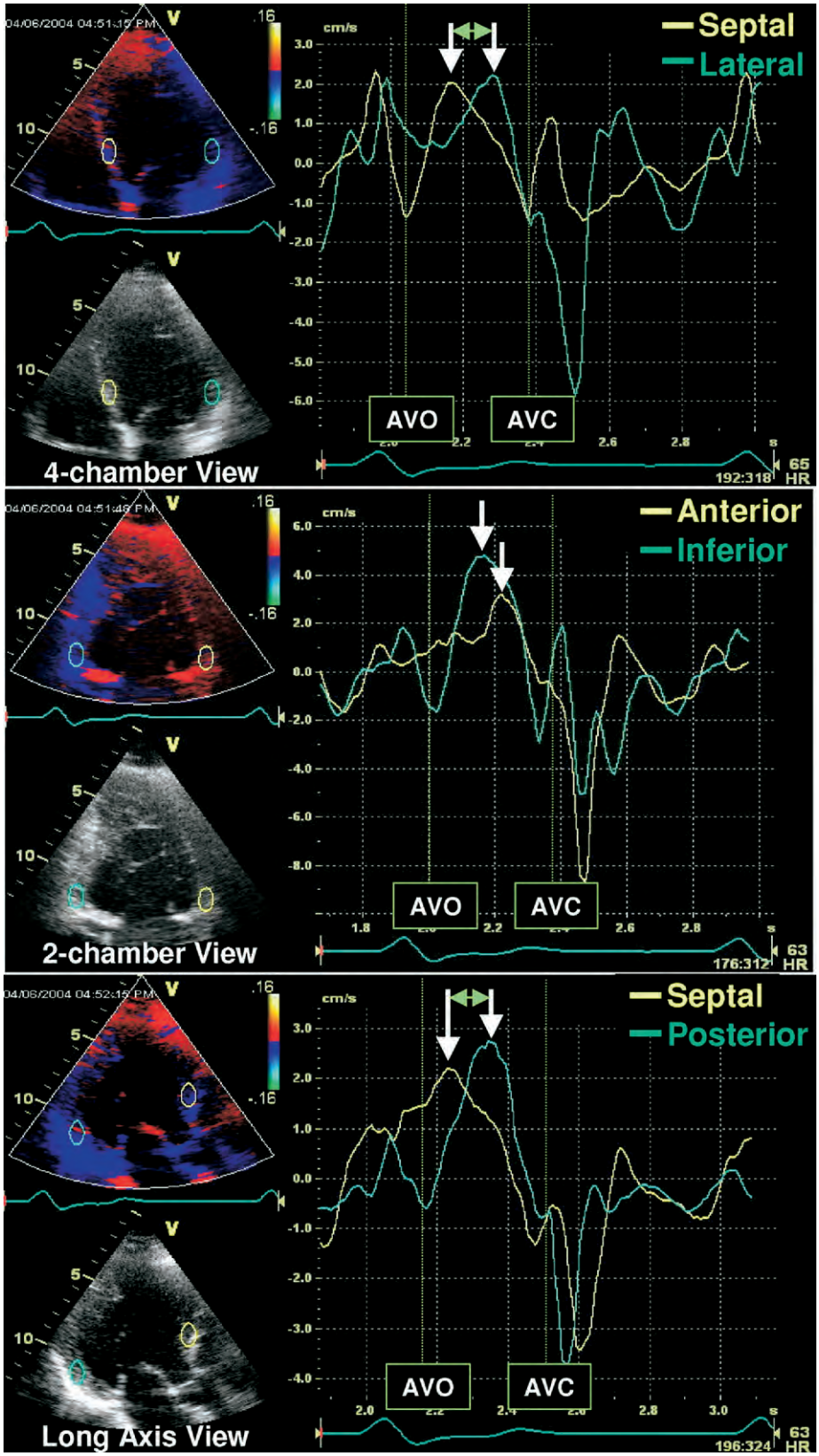

Figure 3 Color-coded tissue Doppler study from 3 standard apical views of patient who responded to resynchronization therapy. Time-velocity curves from representative basal or midlevels are shown. Maximum opposing wall delay was seen in apical long-axis view of 140 milliseconds between septum and posterior wall, consistent with significant dyssynchrony (≥65 milliseconds).

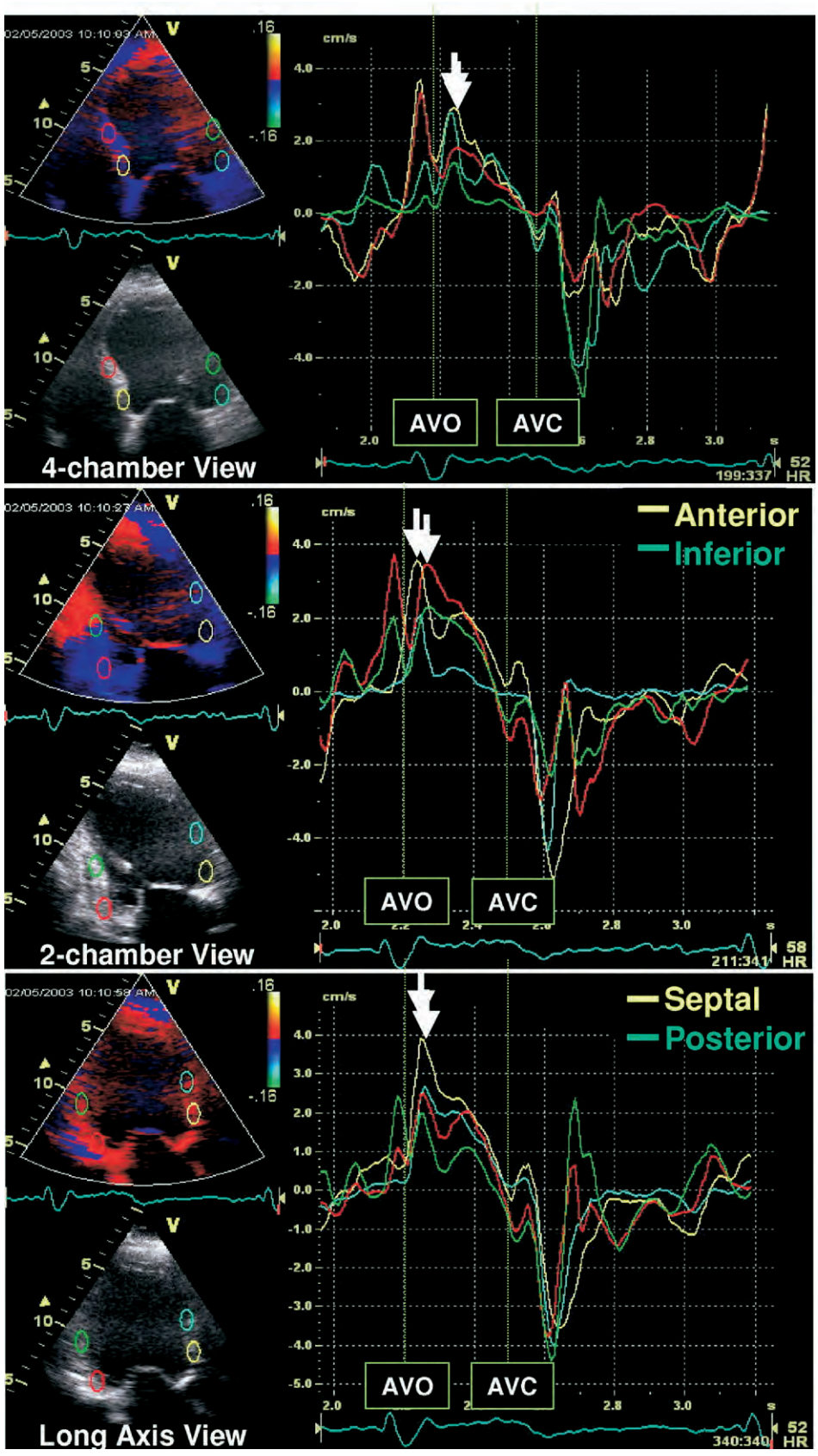

Figure 4 Color-coded tissue Doppler study from 3 standard apical views of patient who did not respond to resynchronization therapy. Time-velocity curves from both basal and midlevels show no significant opposing wall delay less than 65 milliseconds.

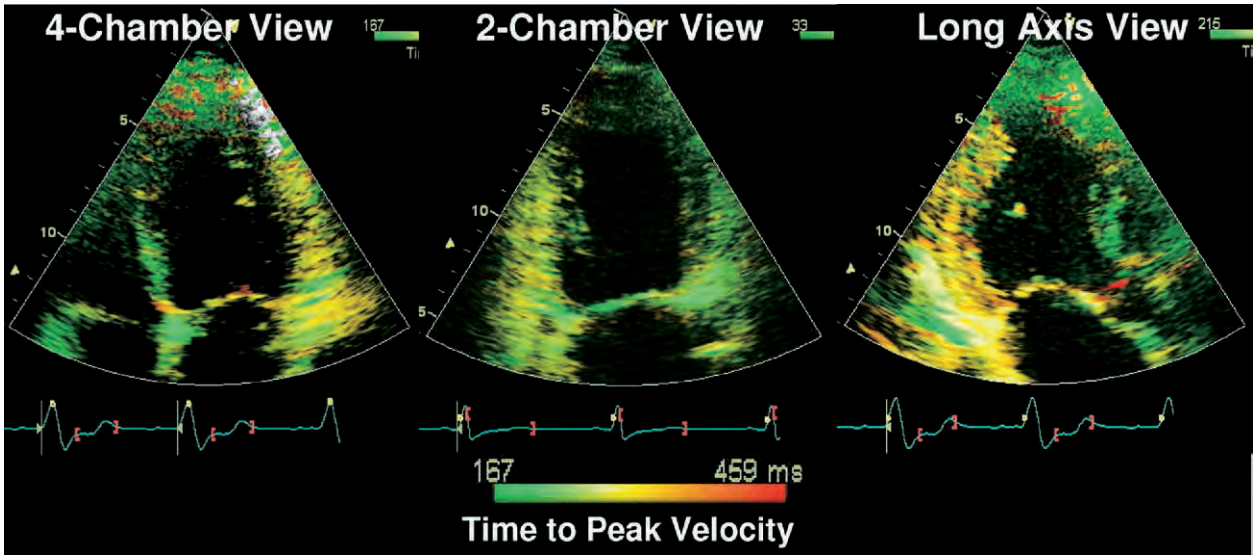

Figure 5 Tissue Doppler study from 3 standard apical views demonstrating color coding of time to peak velocity data from patient with dyssynchrony who responded to resynchronization therapy. Lateral wall (4-chamber view) and posterior wall (apical long-axis views) are color-coded *yellow-orange*, indicating delay in time to peak velocity.

CLINICAL STUDIES USING COLOR TD

The majority of studies have used color-coded TD to assess LV dyssynchrony and predict outcome, and it is the consensus of this writing group that this is currently the preferred approach. The simplest TD approach to identify LV dyssynchrony by color-coded TD uses the basal segments of the apical 4-chamber view to measure the septal-to-lateral delay, known as the two-site method.[15] Subsequently, a 4-segment model was applied that included 4 basal segments (septal, lateral, inferior, and anterior). An opposing wall delay greater than or equal to 65 milliseconds allowed prediction of both clinical response to CRT (defined by an improvement in NYHA class and 6-minute walking distance) and reverse remodeling (defined as a ≥15% reduction in LV end-systolic volume).[15] In addition, patients with LV dyssynchrony greater than or equal to 65 milliseconds had a favorable prognosis after CRT.[15,48] An extension of this opposing wall delay method has included data from the 3 standard apical views: 4-chamber, 2-chamber, and long-axis. The maximum difference in time-to-peak velocity values among the 4 sites from each of the 3 apical views is determined as the maximal opposing wall delay. An important feature of this 3-view model is that it includes the anterior-septum and posterior walls seen in the apical long-axis view, which often has dyssynchrony. Yu et al developed a 12-segment SD model using color TD that also integrates information from the same 3 apical views (4-chamber, 2-chamber, and long-axis).[31,43] The mechanical dyssynchrony index, also known as the Yu index, was derived from calculating the SD of the time-to-peak systolic velocity in the ejection phase 12-site standard deviation.[31,43,49] A 12-site standard deviation cut-off value of greater than or equal to 33 milliseconds was derived from the healthy population to signify mechanical dyssynchrony. To predict LV reverse remodeling (defined as a ≥15% reduction in LV end-systolic volume) in patients with a QRS duration greater than 150 milliseconds, this cut-off value has a sensitivity of 100% and specificity of 78%. For patients with a borderline prolongation of QRS duration of 120 to 150 milliseconds, the sensitivity is 83% and specificity is 86%.[49] An alternate method is to calculate the maximal difference in the time to peak systolic velocity among all segments, where a cut-off value of greater than or equal to 100 milliseconds predicts response to CRT.[31,43] The PROSPECT study reported that the 12-site time-to-peak SD had a lower yield and higher variability than more simple approaches, which illustrates its disadvantage as a more technically demanding approach.[18]

An extension of TD is automated color coding of time-to-peak velocity data. One method is known as tissue synchronization imaging (TSI) (Figure 5). This technology adds a color-coded overlay onto 2D images for a visual identification of regional mechanical delay. Timing should focus on the ejection period and exclude early isovolumic contraction and late postsystolic shortening. Gorcsan et al used TSI color coding to guide placement of regions of interest and assess an antero-septal-to-posterior wall delay greater than or equal to 65 milliseconds from time-velocity curves to predict acute improvement in stroke volume after CRT.[12] Yu et al also used TSI in 56 patients and found the Ts-SD derived by TSI from 12 LV segments had a highest receiver operating characteristic curve area of 0.90. Inclusion of postsystolic shortening in the model significantly reduced the receiver operating characteristic curve area to 0.69. Furthermore, all of the TSI parameters showed a slight, but consistently lower, predictive value than data derived directly from the time-velocity curves.[50] Thus, it is recommended that myocardial time-velocity curves be examined with adjustment of regions of interest as described above to ensure the accuracy of the true peak velocities when TSI is used.

PULSED TD

Pulsed TD has been described as a means to assess dyssynchrony and is available on most echocardiography systems (Figure 6). Briefly, pulsed TD presets must be optimized on the echocardiographic system as recommended by the individual manufacturers. The general approach is as described above in the step-by-step color TD data acquisition and analysis sections, with modifications. The pulsed sample volume is set to approximately 1-cm length, the velocity scale set to maximize the time-velocity curve, and the

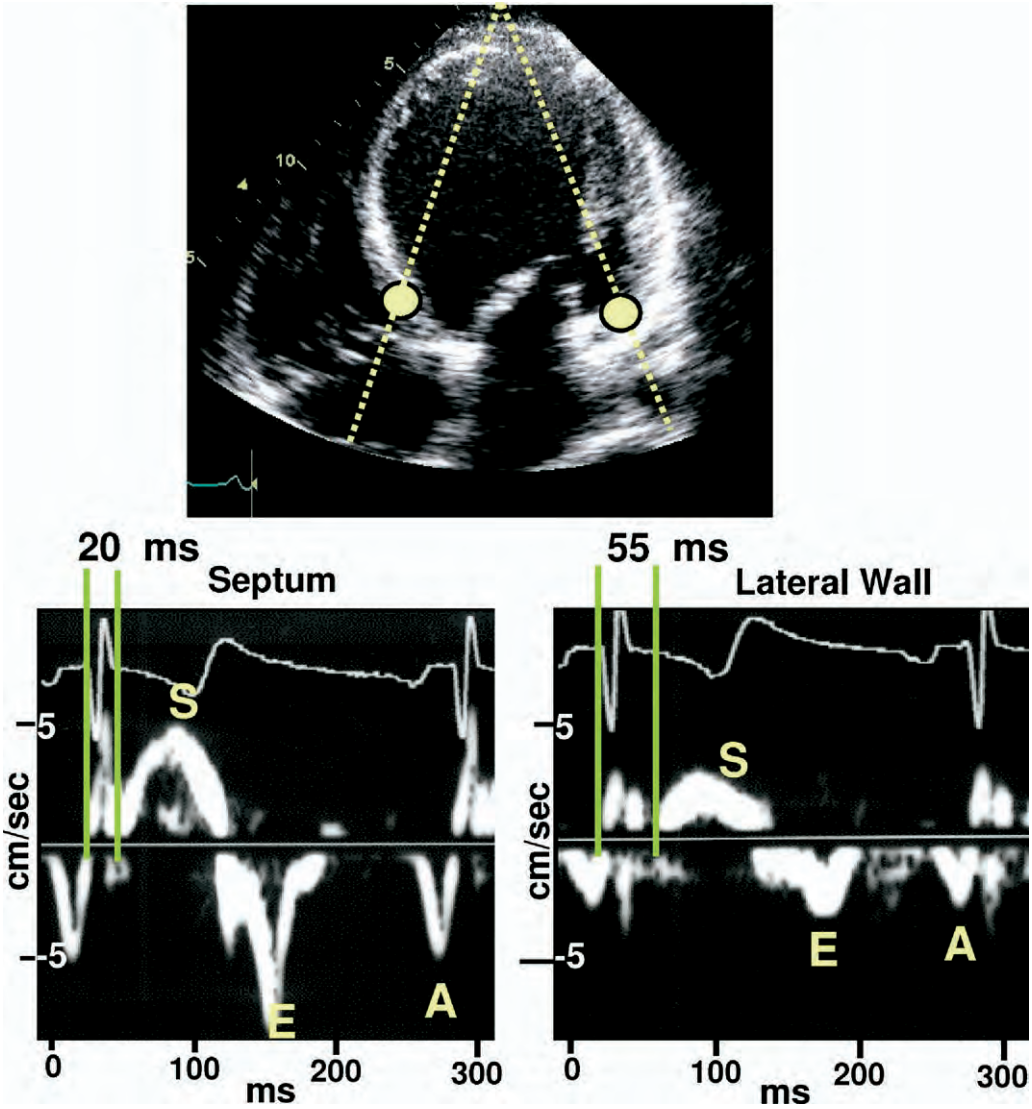

Figure 6 Pulsed tissue Doppler demonstrating dyssynchrony with delayed time to onset systolic velocity in lateral wall, as compared with septum in patient with left bundle branch block before resynchronization therapy.

sweep speed set to 50 to 100 mm/s. Unlike offline color TD data analysis, the step where the sample volume is moved within the segment to search for a reproducible time-velocity signal must be done online. This is a major disadvantage of pulsed TD because it is time-consuming and susceptible to influences of breathing, patient movement, and alterations in heart rate. In addition, the timing of the ejection interval must be transferred manually. Furthermore, the peak velocity may be difficult to identify because of a broad spectral display with a plateau during systole. Because of these technical limitations, color-coded TD is the approach preferred by this writing group. Currently, clinical studies of pulsed TD to predict response to CRT are less numerous than those using color TD. Penicka et al used pulsed wave TD to measure the time of onset of the systolic signal of basal segments from the apical 4-chamber and long-axis views and the lateral right ventricular (RV) wall.[51] Using a composite index of interventricular and intraventricular dyssynchrony longer than 100 milliseconds, they achieved 88% accuracy in identifying all but 6 patients who responded to CRT.

TD LONGITUDINAL STRAIN, STRAIN RATE, AND DISPLACEMENT

Strain and strain rate imaging have the theoretic advantage of differentiating active myocardial contraction or deformation from passive translational movement and have been utilized to identify dyssynchrony.[40,42,52] Longitudinal strain is calculated linearly from TD velocity data as percent shortening (Figure 7). However, TD longitudinal strain can be technically challenging because strain is calculated along scan lines, is Doppler angle dependent, and is difficult in patients with spherical LV geometry, often encountered in severe heart failure. Comparing myocardial velocities and strain rate, Breithardt et al found an association between regional myocardial motion (expressed by velocity parameters) and deformation (expressed by strain rate imaging parameters).[52] They concluded that the degree of dyssynchrony was not completely represented by the timing of myocardial velocity, particularly in ischemic heart disease, and that the timing of deformation should be the preferred modality. Sogaard et al found that the extent of delayed

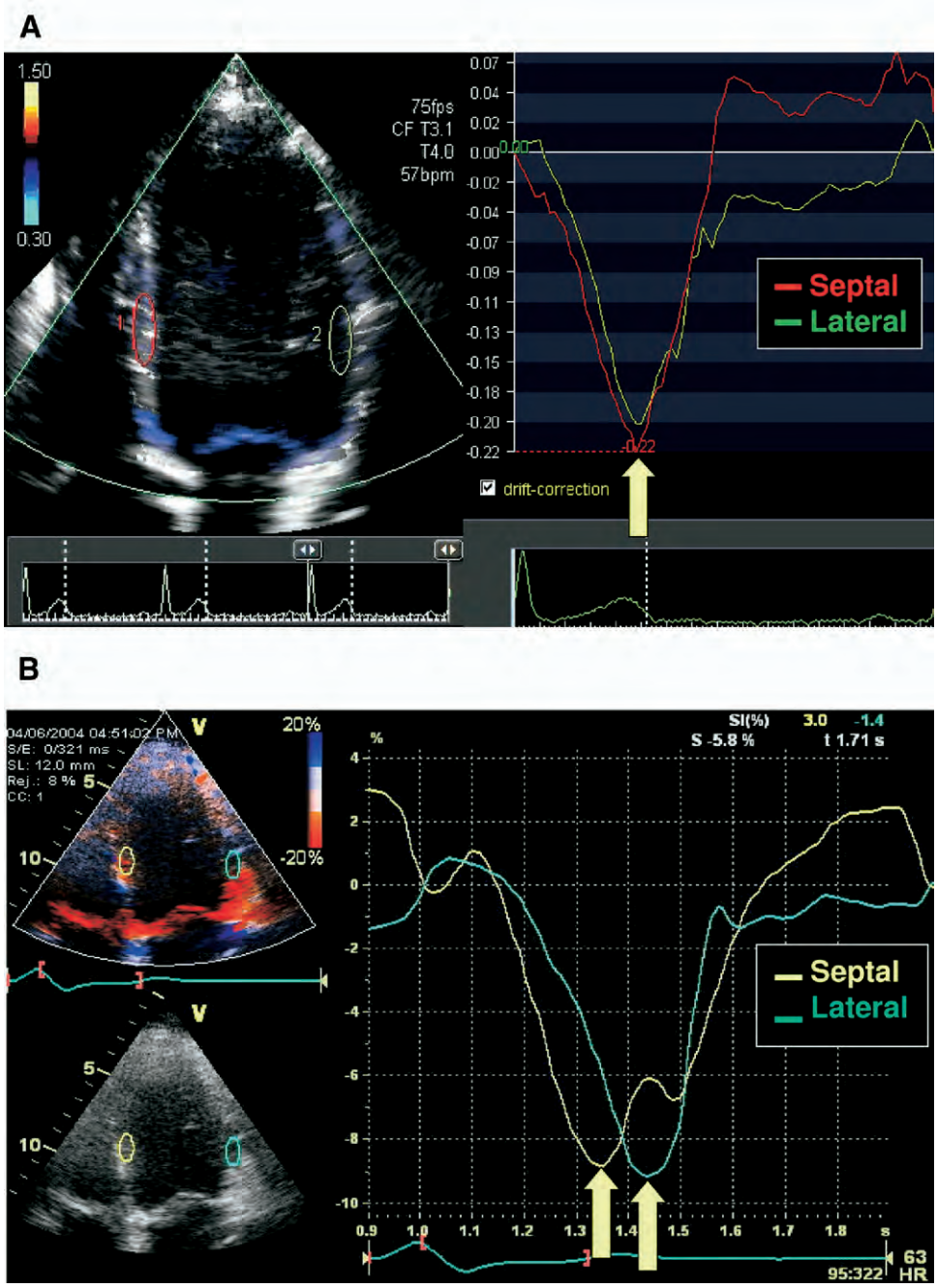

Figure 7 Doppler tissue images demonstrating longitudinal strain in healthy synchronous patient (**A**) and in patient with left bundle branch block before (**B**) resynchronization therapy.

longitudinal contraction at the base predicted improvement in EF after CRT.[41,42] However, Yu et al demonstrated that parameters of strain rate imaging are not useful to predict reverse remodeling response.[43,44,53] Currently, TD strain rate is restricted by a poor signal-to-noise ratio, which adversely affects reproducibility. On the other hand, improvements in strain analysis, including software developments such as strain determined by speckle tracking of routine gray-scale images, are promising as useful markers of systolic dyssynchrony.[54]

Displacement imaging uses TD data to calculate the distance of myocardial movement, and is typically color coded and overlaid onto 2D images. The signal-to-noise ratio is more favorable than strain or strain rate imaging, but displacement is also affected by passive motion, and the Doppler angle of incidence. Improvements in displacement or tissue tracking have been described after CRT, however, cut-off values for predicting response and clinical outcomes after CRT have not yet been established.[42]

RADIAL STRAIN

Because radial thickening is a major vector of LV contraction, and short-axis dynamics are important markers of dyssynchrony,[55] it is

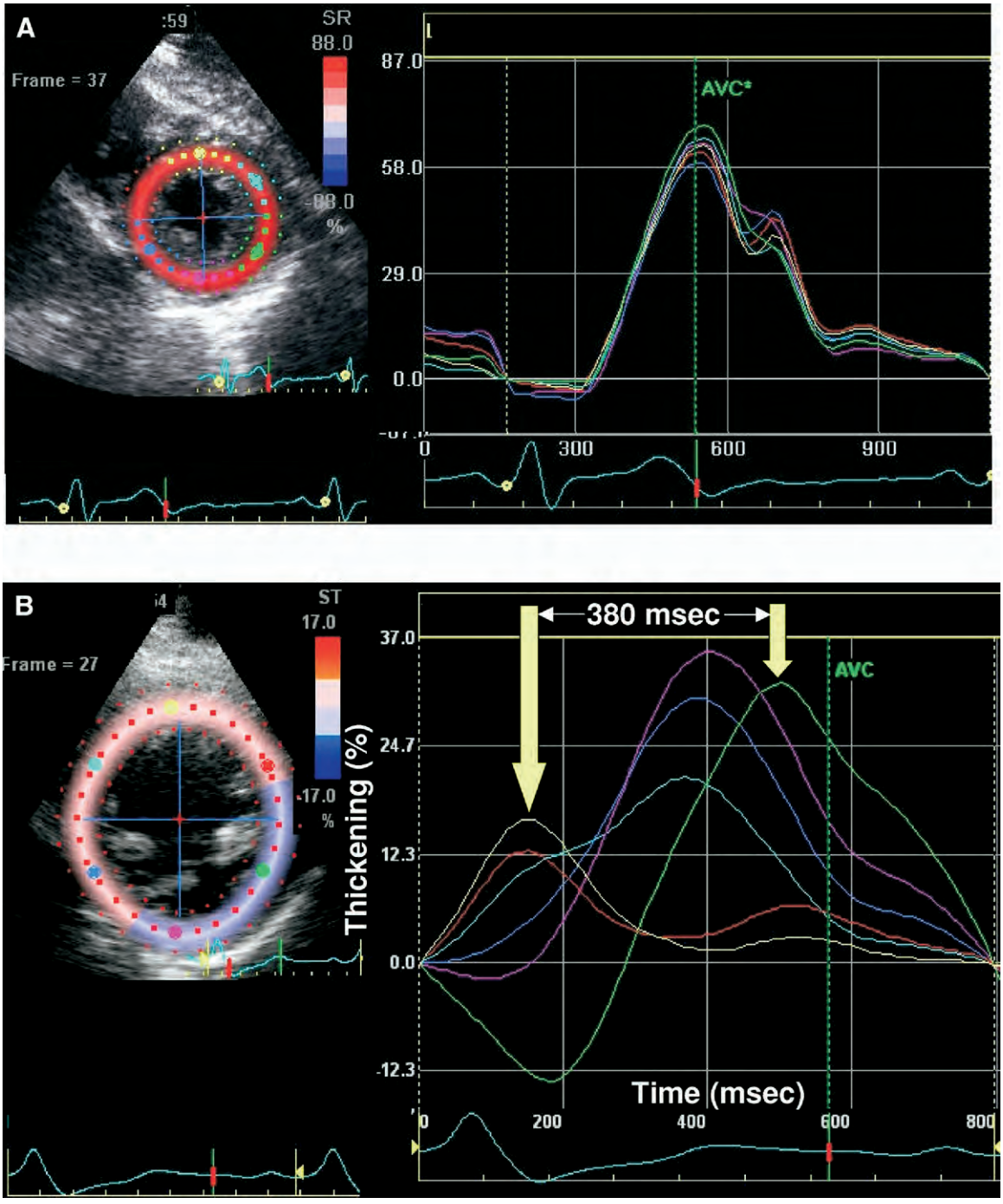

Figure 8 Speckle-tracking images demonstrating synchrony of peak segmental radial strain in healthy individual (**A**) and severe dyssynchrony in patient with heart failure and left bundle branch block (*LBBB*) referred for resynchronization therapy (**B**).

reasonable to utilize this information in a comprehensive examination. Strain has an advantage over M-mode of differentiating active from passive motion and identifying radial mechanical activation.[56] Dohi et al first used TD strain to quantify radial mechanical dyssynchrony in 38 patients who underwent CRT.[57] Radial strain was calculated from TD velocity data from the anteroseptum and posterior wall in the mid LV short-axis view.[58] Disadvantages of TD radial strain included signal noise without adequate image quality and the effect of the Doppler angle of incidence.

A more recent approach is application of a speckle-tracking program that is applied to routine gray-scale echocardiographic images, which is not limited by Doppler angle of incidence. Suffoletto et al studied 64 patients undergoing CRT.[54] Speckle tracking applied to routine midventricular short-axis images determines radial strain from multiple points averaged to 6 standard segments (Figure 8). Baseline speckle-tracking radial dyssynchrony (defined as a time difference in peak septal to posterior wall strain $\geq$ 130 milliseconds) predicted a significant increase in LV EF, with 89% sensitivity and 83% specific-

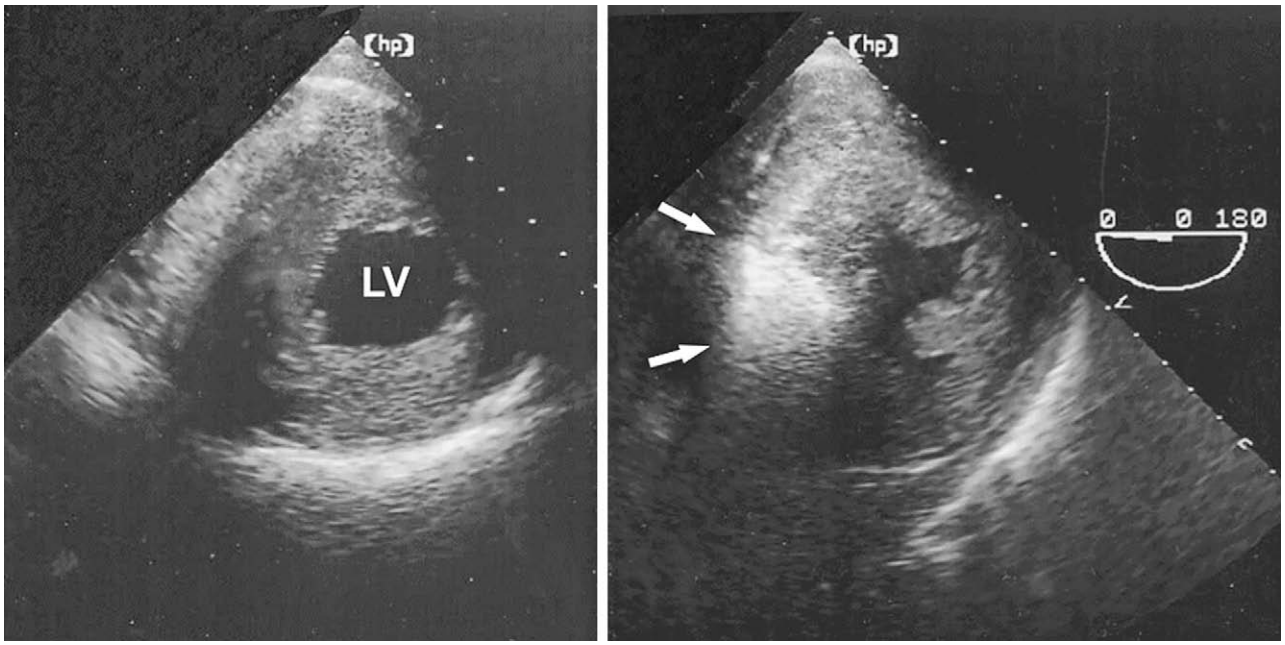

Figure 10 TEE. Transgastric short-axis view before *(left)* and after *(right)* the injection of ultrasound contrast *(arrows)* demonstrating the site of perfusion of the selected septal perforator. Ultrasound contrast is used not only to define the desired perfusion area of the target septal perforator but also to exclude perfusion of unwanted areas, such as the papillary muscles, the distal (apical) portion of the ventricular septum, and the right ventricle. This transgastric short-axis view is particularly useful to delineate the papillary muscles. *LV*, Left ventricle.

inflated balloon catheter under continuous TTE or TEE. The echocardiographic contrast agent should be diluted with normal saline to optimize myocardial opacification and to minimize attenuation. Details of the dilution vary with the contrast agent used. Agitated radiographic contrast can be used instead of an ultrasound contrast agent (Figure 9).

The optimal target territory of the basal septum should include the color Doppler–estimated area of maximal flow acceleration and the area of systolic anterior motion–septal contact without contrast opacification of any other cardiac structures (Figures 9-11). After myocardial contrast echocardiography confirms that the presumed target septal perforator perfuses the desired region of the basal septum, alcohol can be administered.

If TTE is used, apical 4-chamber and 3-chamber (long-axis) views should be used. These views may be supplemented with parasternal long-axis and short-axis views. If TEE is used, the apical 4-chamber view (at 0°) and the longitudinal view (usually 120°-130°) should be used. These views may be supplemented by the transgastric short-axis view to help ensure that no erroneous perfusion of the papillary muscles occurs. The deep transgastric view, which resembles an apical 4-chamber transthoracic view, is useful for measuring the intracavitary gradient with TEE.

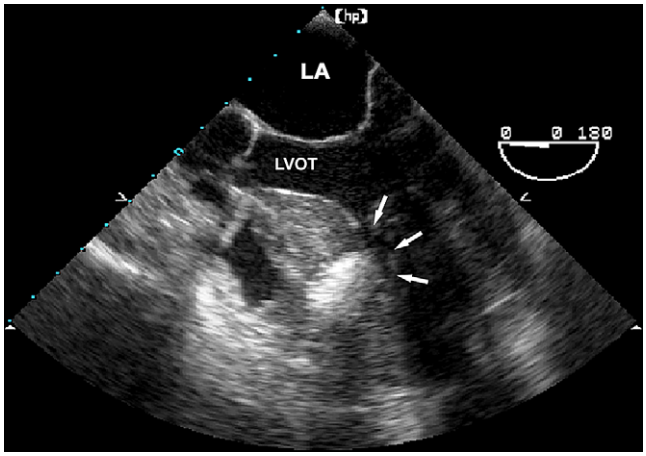

Figure 11 TEE. Midesophageal 4-chamber view after the injection of contrast *(arrows)*, demonstrating that the site of perfusion of the selected septal perforator is too apical and therefore not related to the point of septal contact of the mitral valve. *LA*, Left atrium; *LVOT*, left ventricular outflow tract.

C. Immediate Assessment of Results

Intraprocedural echocardiography is also useful for evaluating the results of the procedure in the catheterization laboratory.[103,105,106] The region of the basal septum, which is infarcted by the infused alcohol, is typically intensely echo dense. In addition, this region of the septum should have reduced thickening and contractility.[103] There should also be resolution or improvement of the degree of systolic anterior motion of the anterior mitral leaflet and usually reduction in the degree of MR. In addition, there should be elimination or reduction of the intracavitary gradient. This is readily measured by TTE and can often be measured by TEE with a deep transgastric view or midesophageal long-axis view.

D. Outcome Data

Several studies have suggested a favorable impact of echocardiographic monitoring during this procedure.[102,105,107] Echocardiographic monitoring of percutaneous transluminal septal myocardial

ablation has resulted in the reduction of the amount of injected alcohol and the number of occluded septal branches.[102] Online echocardiography may also reduce the need for repeat interventions with occlusions of several septal branches, thus avoiding unnecessary enlargement of the septal scar with all of the associated potential negative consequences for left ventricular systolic and diastolic function.

Another important advantage of myocardial contrast echocardiography during the procedure is that opacification of myocardium distant from the intended target septal area can prevent erroneous instillation of alcohol into unwanted territory, such as the papillary muscle, left ventricular free wall, or right ventricle (Figure 11).

A recent American College of Cardiology and European Society of Cardiology consensus document on HOCM stated that "myocardial contrast echocardiography guidance…is important in selecting the appropriate septal perforator branch."[108,109] Nevertheless, a randomized multicenter study with respect to this issue does not exist.

Echocardiography is recommended in selecting the appropriate septal perforator during alcohol injection during septal ablation for HOCM. Both TTE and TEE can be used. They provide an assessment of immediate procedural results and allow monitoring for complications.

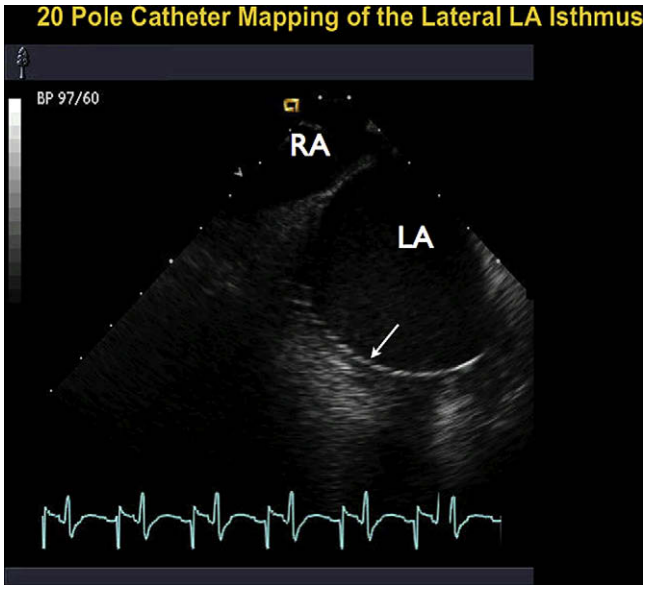

Figure 12 ICE. Phased-array ICE of long-axis view of the left atrium (LA) from the right atrium (RA). Shown is the catheter-tissue contact of a 20-electrode catheter positioned along the posterior mitral annulus *(arrow)*.

X. INTRACARDIAC ECHOCARDIOGRAPHY AND CARDIAC ELECTROPHYSIOLOGY

A. Anatomy-Dependent Arrhythmias

Catheter-based ICE has been applied extensively in cardiac electrophysiology laboratories to guide ablative procedures. To a large degree, this early adoption has occurred because of the critical dependence of specific cardiac arrhythmias on underlying anatomy. For example, accessory atrioventricular pathways bridge from atrial to ventricular tissue across the mitral or tricuspid annulus, requiring selective energy delivery at a specific anatomic location to successfully eliminate related supraventricular tachycardias. In addition, clarification of the pathophysiology of typical atrial flutter demonstrated that the cavotricuspid isthmus was a critically important component of the underlying reentrant circuit.[110,111] Because of this, the nomenclature of this arrhythmia was changed to "isthmus-dependent, counterclockwise atrial flutter." It follows that the ability to visualize specific anatomic structures should be of substantial importance in the nonpharmacologic treatment of these arrhythmias.

B. Phased-Array Imaging

The application of phased-array technology with a transesophageal probe was shown in early studies to be useful for imaging during VT ablation[112] and the treatment of accessory pathway–mediated tachycardias.[113-115] The miniaturization of this technology and application via intracardiac catheters allowed deeper penetration and standard 2D visualization and Doppler imaging of both right-sided and left-sided structures from within the right heart.[116] Long-axis imaging with phased-array technology has been particularly suited for the electrophysiology laboratory environment. Within the context provided by forward imaging, intracardiac ultrasound frequently has been used to guide the insertion of catheters into specific cardiac chambers, across the cardiac valves into the ventricles, and to guide transseptal catheterization into left-heart structures, from a single imaging viewpoint or with minimal catheter rotation. Intracardiac ultrasound has been preferable to transesophageal imaging because it does not require prolonged esophageal intubation, accompanying patient discomfort, or the risk for aspiration. It is also routinely performed by a single interventionist, without the need for other personnel for further image acquisition and interpretation.

C. Ultrasound-Guided Anatomic Ablation

Intracardiac ultrasound has been applied to guide the positioning of ablation catheters near specific cardiac structures for ablation of the related arrhythmia, as seen in Figure 12. The value of such intracardiac echocardiographic imaging extends to establishing a clear-cut relationship between the catheter tip and underlying tissue, a critically important determinant of ablation success. In many cases, the lesion produced in the delivery of ablation energy can be visualized in tissue adjacent to the catheter tip. This observation is of theoretical importance, because the identification of each individual lesion could facilitate the juxtaposition of subsequent energy deliveries, as required in linear ablation. This utility has also been documented in linear ablation studies from several centers.[21,117-119] However, the visualization of an evolving lesion is a function of the imaging frequency, the distance of the ablation site from the transducer, the catheter tip–tissue contact, the delivered energy, and the thickness of the underlying tissue. Therefore, the lesions formed by the ablation of ventricular myocardium are more readily seen than with atrial ablation.[120-122] Furthermore, continued energy delivery in the ablation of atrial tissue to the point of lesion visualization is not necessary for a successful outcome and may be excessive. In short, lesion visualization with B-mode imaging is insufficiently sensitive for establishing an end point for ablation. Other means of enhancing lesion detection are currently being studied.[123]

Avariety of studies have tested the utility of intracardiac ultrasound in the setting of atrial tachycardias,[124] atrioventricular nodal reentrant tachycardia,[125] sinus tachycardia,[126] ventricular arrhythmias,[127] atrial flutter,[110,121,128,129] and AF.[18,21,22,24,130] Ablation of the cavotricuspid isthmus has been found to be 95% to 98% successful in eliminating atrial flutter simply through the identification of the anatomic site of origin of that arrhythmia.[110,111] Recent studies[131,132] have also shown

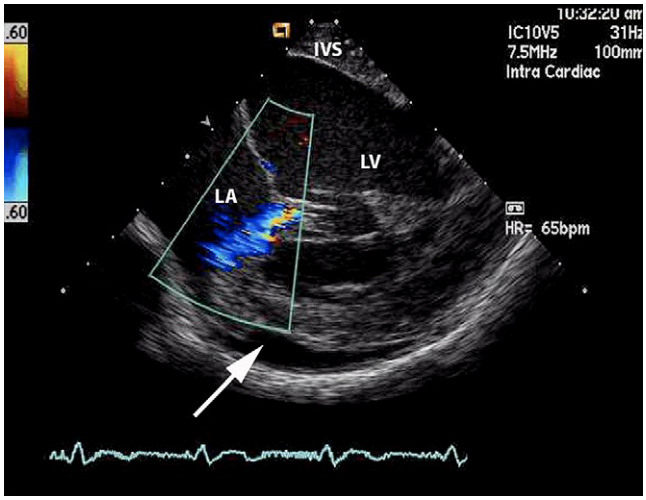

Figure 13 ICE. Phased-array ICE from the right ventricle. Imaging through the interventricular septum (IVS) to display the left ventricle (LV) and left atrium (LA) demonstrates an emerging pericardial effusion *(arrow)* during an ablation procedure. MR is also shown by color Doppler mapping.

the utility of imaging the left ventricular scar that results from myocardial infarction in ablation of postinfarct VT. Typically, stable VT arises within the border zone of an infarct. In such cases, intracardiac ultrasound can be used to guide ablation and create lesion bridges from the center of the scar, across the infarct border zone, on to a neighboring electrically inert cardiac structure such as the mitral annulus. Such lesions interrupt the VT circuit that passes through the spared tissue immediately around the infarct, such as the submitral valve isthmus in the setting of inferior wall infarction.[133] Linear ablation along the border of an infarction, such as is required for ablation of fast, unstable VT, has also been facilitated by direct imaging.[131] Such left ventricular imaging is best conducted from below the tricuspid valve from a venue near the right ventricular outflow tract. From this position, both long-axis and short-axis images of the left ventricle can be created.[116]

D. Ablation of AF

ICE has been used most consistently for the guidance of ablation of AF. This approach establishes the number and position of pulmonary veins and determines whether a left pulmonary vein antrum, formed by the confluence of the left superior and inferior pulmonary veins, is present. ICE also clarifies the branching patterns of the right pulmonary vein, guides the positioning of interventional catheters, verifies catheter tip–tissue contact, assesses underlying pulmonary vein physiology, helps in the positioning of balloon-type catheters for ablative interventions, and monitors for excessive tissue heating as manifested by the occurrence of microbubbles. Furthermore, ultrasound establishment of the venoatrial junction has recently been shown in preliminary studies to be more accurate than is possible with contrast venography.[134,135] Given its position in relationship to the left pulmonary veins, the location of the vein of Marshall, relevant in AF ablation, can also be identified from imaging of the "Q-tip" ridge, seen between the LAA and those pulmonary veins.[136]

Not only does the ultrasound beam allow identification of the underlying pulmonary vein and other relevant structures, it also enables positioning of guidance catheters, such as the circular Lasso catheter, to a position immediately at the orifice of the pulmonary vein. This is particularly critical because these catheters have a tendency to drift into the vein, providing a false sense of the true orifice of the vessel.[137] Ablation too far into a vein increases the risk for pulmonary vein stenosis and decreases the efficacy of AF ablation.[138] Several studies[18,22,130,139,140] have shown the utility of intracardiac ultrasound to guide ablation at or outside the pulmonary vein orifice, which results in increased efficacy for AF ablation.

E. Monitoring for Ablation-Related Complications

Microbubble formation has also been widely observed with intracardiac ultrasound imaging.[21,141,142] This phenomenon may be even more accurate than catheter-tip temperature monitoring for the assessment of heat generation during the ablation of cardiac tissue.[142,143] Nevertheless, although this finding has been proposed as an end point to guide ablation, recent studies have demonstrated that microbubble appearance frequently reflects excess tissue heating to substantially greater temperatures than reflected by catheter-tip temperature monitoring.[139,141] This inadvertent tissue overheating, in turn, may lead to clot, char, or crater formation; intracardiac thrombus; or even pulmonary vein stenosis. Therefore, ultrasound visualization of microbubbles is most useful for prompting discontinuation of energy delivery when microbubbles are seen.

Along this same line, intracardiac ultrasound is useful in monitoring for potential complications of ablative intervention. In addition to the observation of the untoward results of tissue overheating, several studies have recently demonstrated the utility of ultrasound for detecting thrombus formation on the interventional catheter, which could lead to either a stroke or a peripheral thromboembolic event.[144,145] Ongoing surveillance of the pericardium during an interventional case is useful for the early detection of an effusion (Figure 13), before its physiological relevance is manifested by tamponade physiology. Imaging from an intracardiac venue also facilitates the catheter-based treatment of the effusion.

Doppler imaging likewise has contributed in the surveillance process. Pulsed-wave Doppler imaging, available with phased-array imaging over the course of an ablation, reveals an increase in flow velocity with pulmonary vein narrowing. An increment to a level in excess of 1.6 m/s has been found to be predictive of subsequent stenosis.[146] In contrast, veins with lower flow velocities, $\leq$1.0 m/s, are unlikely to progress to any significant degree.[147] It is noteworthy, however, that these intracardiac Doppler flows are highly dependent on the presence of AF or catecholamines.[148]

ICE is recommended for radiofrequency ablation for AF. It is used to guide transseptal catheterization, as well multiple aspects of the procedure, to monitor for complications, and to assess pulmonary vein flow before and after ablation.

XI. FUTURE DIRECTIONS

A. Echocardiography in Complex Mitral Valve Procedures (Investigational Devices)

Newer investigational percutaneous mitral valve repair systems are being developed as an alternative to surgical repair for MR, either using the concepts of the edge-to-edge repair technique developed by Alfieri et al[149-151] but performed with a percutaneous endovascular repair system[152-158] or by the performance of a percutaneous mitral annuloplasty repair with a device placed in the coronary sinus or at the level of the mitral annulus. A variety of delivery approaches for these devices have been proposed. For example, an endovascular mitral repair system uses a steerable guide catheter to precisely

manipulate and position a clip that approximates the middle anterior and posterior leaflet scallops of the mitral valve, thus reducing or eliminating MR.[155] This system is currently being investigated in humans in phase I and II trials. Additional percutaneous mitral repair devices that use the concept of edge-to-edge repair are also being developed.

The delivery of the percutaneous edge to edge mitral valve repair system has 5 steps that require echocardiographic guidance: transseptal catheterization, alignment of the clip delivery system perpendicular to the plane of the mitral valve and centered with reference to the line of coaptation, alignment of the clip with the open arms perpendicular to the coaptation line of the mitral valve, closing of the arms and approximation of the tips of the mitral valve, and release of the implant device. A combination of TEE and supplemental TTE has been used to guide the procedure.

Other coronary sinus and mitral annular devices are also being developed to perform percutaneous mitral annuloplasty repair, thereby reducing MR by enhancing mitral coaptation. TEE or ICE can be used to guide cannulation of the coronary sinus ostium, place the device, monitor for procedural complications, and assess the degree of MR and transmitral gradients before and after the procedure.

B. Role of Echocardiography in the Placement of LAA Occluders (Investigational Devices)

The majority of thromboemboli in AF arise in the LAA.[159-161] That observation led to the hypothesis that functional obliteration of the LAA could prevent stroke. For this reason, surgeries for several indications often include prophylactic intraoperative ligation of the LAA,[162,163] and some have recommended LAA ligation in all patients having cardiac surgery, regardless of the indication.[164]

A percutaneous transcatheter approach for the prevention of cardioembolic stroke in patients with AF has been proposed, by the placement of an implantable prosthetic device that seals that the communication between the LAA and the left atrium. Initial testing in animals[31] and humans[165] and, more recently, anatomic and hemodynamic data[166] have suggested successful occlusion and stroke prevention. A percutaneous LAA transcatheter occlusion device was the first device tested in humans; ultimately, the trials of this first device were halted because of increased morbidity and mortality. TEE had been used in all published human trials of this device. A newer device has been described.[167] This nitinol metal device is designed to be placed in the LAA via a percutaneous transcatheter approach by a standard transseptal approach with fluoroscopic and TEE guidance. TEE is important in sizing the ostium of the LAA and selecting an appropriately sized device for implantation.

After device release, TEE is repeated to confirm the proper deployment of the device and to assess for procedural complications. The device is examined for stability and leakage. Atrial septal examination is performed to look for an ASD; a small residual defect is common after the procedure. The pericardium is reevaluated for effusion.

C. 3D Echocardiography

A new application of echocardiography, 3D imaging, offers the potential to contribute significantly to interventional procedures. For example, myocardial biopsy has been performed with 3D imaging as a guide for bioptome position (as opposed to the standard approach with fluoroscopy). In one study of 63 routine right ventricular biopsy procedures in cardiac allograft recipients, 3D imaging was deemed feasible, and improved localization of the bioptome was observed, with the potential to improve cardiac biopsy efficacy and safety.[168]

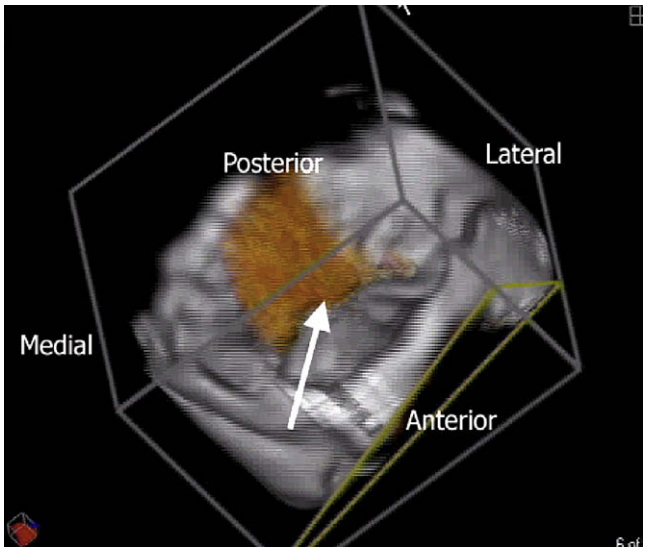

Figure 14 TEE. Reconstructed 3D image of the left atrial surface of the mitral valve in a patient with severe MR originating from nearly the entire mitral coaptation surface (*arrow* indicating red flow into the left atrium on color mapping). Anatomic coordinates are indicated for reference.

Mitral valve anatomy may be better studied with 3D imaging than with 2D imaging (Figure 14), and therefore, 3D imaging can play a significant role in the planning of surgical or percutaneous approaches to mitral valve repair[169-171] (Figure 15). Human studies with intraoperative 3D TEE have shown excellent correlation with surgical findings (94% [34 of 36 patients]) in the correct identification of scallop or segment prolapse.[171]

Others have found incremental value from 3D TEE and TTE over 2D echocardiography for the selection of appropriate patients and the accurate visualization of postprocedural commissural splitting and leaflet tears in patients undergoing PBMV.[172,173] Similarly, it is expected that 3D echocardiography will play a role in the planning of percutaneous mitral repair of MR, such as that shown in Figure 16.[174]

The use of percutaneously delivered devices for ASD or PFO repair is increasing. Three-dimensional imaging allows for accurate anatomic assessment before the procedure and can localize the closure device during the procedure in relation to other cardiac structures, potentially enhancing success and possibly decreasing the complication rate.[175] In 40 of 41 patients (98%) undergoing device ASD closure, 3D images of defects were obtained, and these images more accurately assessed ASD size (using balloon sizing as the "gold standard") than did 2D TEE. Additionally, device position was more accurately assessed with 3D imaging.[176] Real-time 3D echocardiography has also been used for accurate assessment of the morphology and efficacy of transcatheter devices used for ASD and PFO closure.[177] In 4 patients who underwent percutaneous closure of ASDs or PFO (3 ASDs, 1 PFO), real-time 3D echocardiography provided comprehensive anatomic assessment of ASD and PFO closure devices.[177]

Interventional approaches for the treatment of patients with HOCM are also increasing.[101] Real-time 3D echocardiography has also been successfully used to guide the surgical approach to myectomy and mitral valve repair in 10 patients in whom a "surgeon's view" by 3D echocardiography allowed refinement of the planned surgical approach.

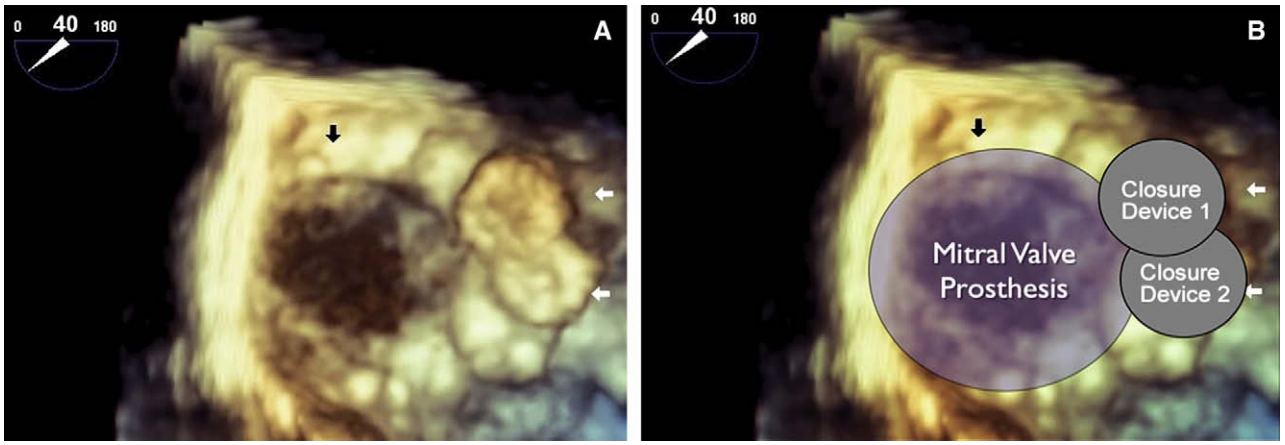

Figure 15 Three-dimensional TEE. **(A)** Three-dimensional image of a mitral bioprosthesis *(black arrow)* and two closure devices *(white arrows)* used to close paravalvular MR. **(B)** Explanatory overlays added. The perspective is from the left atrium. It is often difficult to identify the exact site of regurgitation and also to guide interventional devices to the correct location when repairing paravalvular regurgitation using occluder devices. In this case, real time 3D imaging was critical in positioning the closure devices and defining the location and extent of the paravalvular jet.

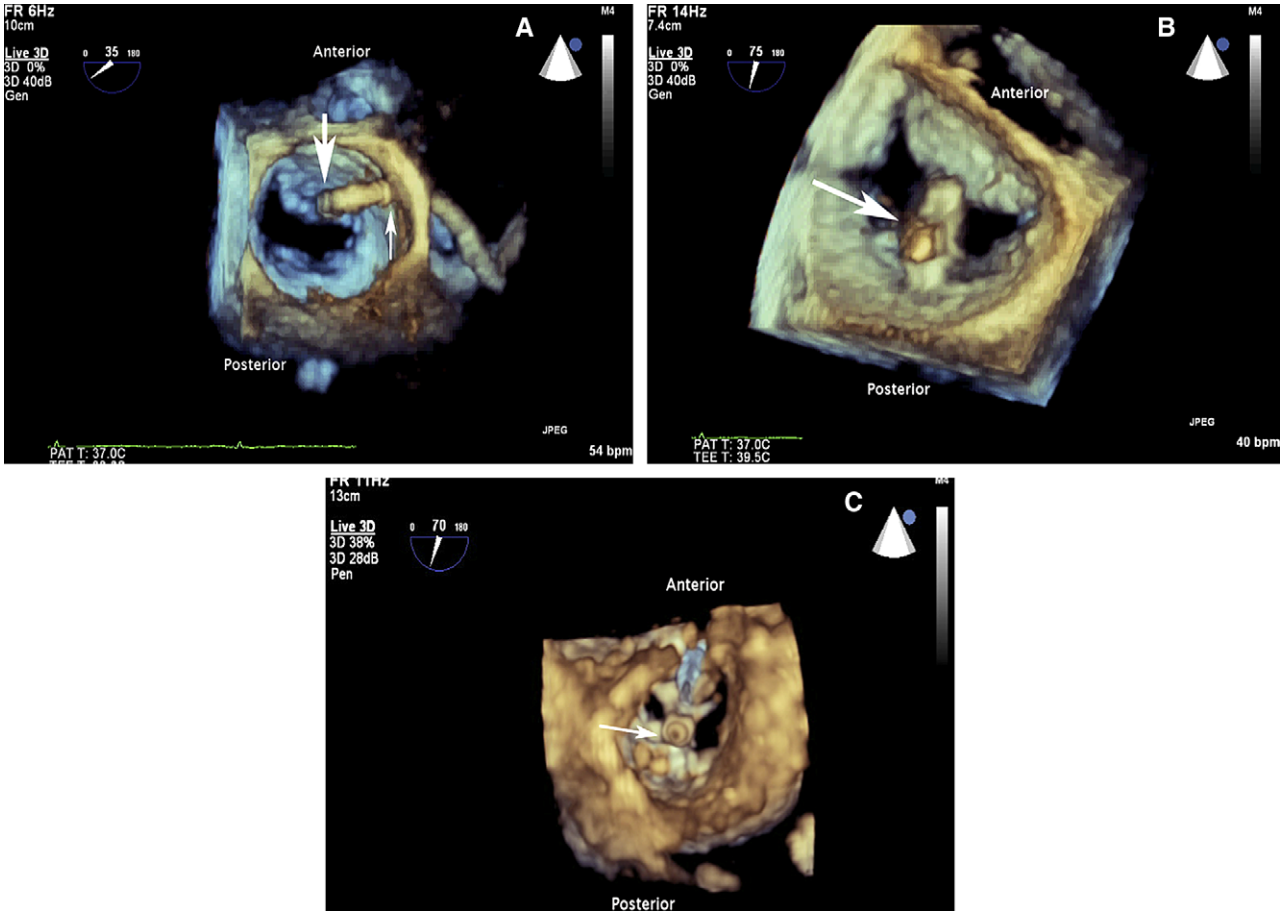

Figure 16 Three-dimensional TEE. Percutaneous edge-to-edge repair of MR using a clip. **(A)** Percutaneous clip being aligned over the mitral valve in the left atrium. The *large arrow* indicates a clip prior to opening, and the smaller arrow indicates a guide catheter tip. **(B)** The open ''arms'' of the prosthesis *(arrow)* as they are aligned perpendicularly to the line of coaptation prior to grasping of the leaflets. **(C)** Imaging from the left ventricle perspective demonstrates a closed clip *(arrow)* creating a double-orifice mitral valve repair.

D. Echocardiography in Percutaneous Aortic Valve Replacement

Recently, percutaneous transcatheter aortic valve replacement has been described, and initial studies are presently being performed with two distinct biologic valves mounted on stents, which are crimped onto a balloon and delivered using a valvuloplasty technique.[178-181] These valves can be percutaneously placed via a retrograde transaortic approach or via a surgical direct transapical approach.[182-184] Echocardiography plays a critical role in patient selection, particularly in choosing the appropriate size of the prosthesis to be implanted. In particular, the aortic annular diameter is important in determining prosthesis size.[182] Small differences in aortic annular diameter and geometry have been demonstrated between TTE and TEE. During the procedure, TEE has been used to help ensure appropriate positioning of the prosthesis and to assess for paravalvular regurgitation after the valve has been implanted. Real-time 3D TEE has also been described during this procedure, but its role and incremental value compared with standard TEE are not fully known at this time.

REFERENCES

1. Pandian NG, Kumar R, Katz SE, Tutor A, Schwartz SL, Weintraub AR, et al. Real-time, intracardiac, two-dimensional echocardiography: enhanced depth of field with a low-frequency (12.5 MHz) ultrasound catheter. Echocardiography 1991;8:407-22.
2. Pandian NG, Schwartz SL, Weintraub AR, Hsu TL, Konstam MA, Salem DN. Intracardiac echocardiography: current developments. Int J Card Imaging 1991;6:207-19.
3. Syracuse DC, Gaudiani VA, Kastl DG, Henry WL, Morrow AG. Intraoperative, intracardiac echocardiography during left ventriculomyotomy and myectomy for hypertrophic subaortic stenosis. Circulation 1978; 58:123-7.
4. Weintraub AR, Schwartz SL, Smith J, Hsu TL, Pandian NG. Intracardiac two-dimensional echocardiography in patients with pericardial effusion and cardiac tamponade. J Am Soc Echocardiogr 1991;4:571-6.
5. Schwartz SL, Pandian NG, Kumar R, Katz SE, Kusay BS, Aronovitz M, et al. Intracardiac echocardiography during simulated aortic and mitral balloon valvuloplasty: in vivo experimental studies. Am Heart J 1992; 123:665-74.
6. Schwartz SL, Pandian NG, Hsu TL, Weintraub A, Cao QL. Intracardiac echocardiographic imaging of cardiac abnormalities, ischemic myocardial dysfunction, and myocardial perfusion: studies with a 10 MHz ultrasound catheter. J Am Soc Echocardiogr 1993;6:345-55.
7. Hung JS, Fu M, Yeh KH, Wu CJ, Wong P. Usefulness of intracardiac echocardiography in complex transseptal catheterization during percutaneous transvenous mitral commissurotomy. Mayo Clin Proc 1996;71: 134-40.
8. Tardif JC, Vannan MA, Miller DS, Schwartz SL, Pandian NG. Potential applications of intracardiac echocardiography in interventional electrophysiology. Am Heart J 1994;127:1090-4.
9. Miyamoto N, Kyo S, Motoyama T, Hung J-S, Suzuki S, Aihara S, et al. Usefulness of intracardiac echocardiography for guidance of transseptal puncture procedure [in Japanese]. J Cardiol 1995;25:29-35.
10. Segar DS, Bourdillon PD, Elsner G, Kesler K, Feigenbaum H. Intracardiac echocardiography-guided biopsy of intracardiac masses. J Am Soc Echocardiogr 1995;8:927-9.
11. Vazquez de Prada JA, Chen M, Guerrero JL, Padial L, Jiang L, Schwammenthal E, et al. Intracardiac echocardiography: in vitro and in vivo validation for right ventricular volume and function. Am Heart J 1996;131:320-8.
12. Sonka M, Liang W, Kanani P, Allan J, DeJong S, Kerber R, et al. Intracardiac echocardiography: computerized detection of left ventricular borders. Int J Card Imaging 1998;14:397-411.
13. Spencer KT, Kerber R, McKay C. Automated tracking of left ventricular wall thickening with intracardiac echocardiography. J Am Soc Echocardiogr 1998;11:1020-6.
14. Bartel T, Konorza T, Arjumand J, Ebradlidze T, Eggebrecht H, Caspari G, et al. Intracardiac echocardiography is superior to conventional monitoring for guiding device closure of interatrial communications. Circulation 2003;107:795-7.
15. Boccalandro F, Baptista E, Muench A, Carter C, Smalling RW. Comparison of intracardiac echocardiography versus transesophageal echocardiography guidance for percutaneous transcatheter closure of atrial septal defect. Am J Cardiol 2004;93:437-40.
16. Rhodes JF Jr, Qureshi AM, Preminger TJ, Tuzcu EM, Casserlyl IP, Dauterman KW, et al. Intracardiac echocardiography during transcatheter interventions for congenital heart disease. Am J Cardiol 2003;92:1482-4.
17. Mullen MJ, Dias BF, Walker F, Siu SC, Benson LN, McLaughlin PR. Intracardiac echocardiography guided device closure of atrial septal defects. J Am Coll Cardiol 2003;41:285-92.
18. Marrouche NF, Martin DO, Wazni O, Gillinov M, Klein A, Bhargava M, et al. Phased-array intracardiac echocardiography monitoring during pulmonary vein isolation in patients with atrial fibrillation: impact on outcome and complications. Circulation 2003;107:2710-6.
19. Jongbloed MR, Bax JJ, de Groot NM, Dirksen MS, Lamb HJ, deRoos A, et al. Radiofrequency catheter ablation of paroxysmal atrial fibrillation: guidance by intracardiac echocardiography and integration with other imaging techniques. Eur J Echocardiogr 2003;4:54-8.
20. Butera G, Chessa M, Bossone E, Negura DG, De Rosa G, Carminati M. Transcatheter closure of atrial septal defect under combined transesophageal and intracardiac echocardiography. Echocardiography 2003;20:389-90.
21. Martin RE, Ellenbogen KA, Lau YR, Hall JA, Kay GN, Shepard RK, et al. Phased-array intracardiac echocardiography during pulmonary vein isolation and linear ablation for atrial fibrillation. J Cardiovasc Electrophysiol 2002;13:873-9.
22. Mangrum JM, Mounsey JP, Kok LC, DiMarco JP, Haines DE. Intracardiac echocardiography-guided, anatomically based radiofrequency ablation of focal atrial fibrillation originating from pulmonary veins. J Am Coll Cardiol 2002;39:1964-72.
23. Calò L, Lamberti F, Loricchio ML, D'Alto M, Castro A, Boggi A, et al. Intracardiac echocardiography: from electroanatomic correlation to clinical application in interventional electrophysiology. Ital Heart J 2002; 3:387-98.
24. Morton JB, Sanders P, Byrne MJ, Power J, Mow C, Edwards GA, et al. Phased-array intracardiac echocardiography to guide radiofrequency ablation in the left atrium and at the pulmonary vein ostium. J Cardiovasc Electrophysiol 2001;12:343-8.
25. Hijazi Z, Wang Z, Cao Q, Koenig P, Waight D, Lang R. Transcatheter closure of atrial septal defects and patent foramen ovale under intracardiac echocardiographic guidance: feasibility and comparison with transesophageal echocardiography. Catheter Cardiovasc Interv 2001;52:194-9.
26. Koenig P, Cao QL, Heitschmidt M, Waight DJ, Hijazi ZM. Role of intracardiac echocardiographic guidance in transcatheter closure of atrial septal defects and patent foramen ovale using the Amplatzer device. J Interv Cardiol 2003;16:51-62.
27. Koenig PR, Abdulla RI, Cao QL, Hijazi ZM. Use of intracardiac echocardiography to guide catheter closure of atrial communications. Echocardiography 2003;20:781-7.
28. Zanchetta M, Onorato E, Rigatelli G, Pedon L, Zennaro M, Carrozza A, et al. Intracardiac echocardiography-guided transcatheter closure of secundum atrial septal defect: a new efficient device selection method. J Am Coll Cardiol 2003;42:1677-82.
29. Zanchetta M, Pedon L, Rigatelli G, Carrozza A, Zennaro M, DiMartino R, et al. Intracardiac echocardiography evaluation in secundum atrial septal defect transcatheter closure. Cardiovasc Intervent Radiol 2003;26:52-7.
30. Johnson SB, Seward JB, Packer DL. Phased-array intracardiac echocardiography for guiding transseptal catheter placement: utility and learning curve. Pacing Clin Electrophysiol 2002;25:402-7.
31. Nakai T, Lesh MD, Gerstenfeld EP, Virmani R, Jones R, Lee RJ. Percutaneous left atrial appendage occlusion (PLAATO) for preventing

cardioembolism: first experience in canine model. Circulation 2002;105: 2217-22.
32. Salem MI, Makaryus AN, Kort S, Chung E, Marchant D, Ong L, et al. Intracardiac echocardiography using the AcuNav ultrasound catheter during percutaneous balloon mitral valvuloplasty. J Am Soc Echocardiogr 2002;15:1533-7.
33. Das P, Prendergast B. Imaging in mitral stenosis: assessment before, during and after percutaneous balloon mitral valvuloplasty. Expert Rev Cardiovasc Ther 2003;1:549-57.
34. Johnston TA, Jaggers J, McGovern JJ, O'Laughlin MP. Bedside transseptal balloon dilation atrial septostomy for decompression of the left heart during extracorporeal membrane oxygenation. Catheter Cardiovasc Interv 1999;46:197-9.
35. Rocha P, Berland J, Rigaud M, Fernandez F, Bourdarias JP, Letac B. Fluoroscopic guidance in transseptal catheterization for percutaneous mitral balloon valvotomy. Catheter Cardiovasc Diagn 1991;23:172-6.
36. Reig J, Mirapeix R, Jornet A, Petit M. Morphologic characteristics of the fossa ovalis as an anatomic basis for transseptal catheterization. Surg Radiol Anat 1997;19:279-82.
37. O'Keefe JH Jr, Vlietstra RE, Hanley PC, Seward JB. Revival of the transseptal approach for catheterization of the left atrium and ventricle. Mayo Clin Proc 1985;60:790-5.
38. Roelke M, Smith AJ, Palacios IF. The technique and safety of transseptal left heart catheterization: the Massachusetts General Hospital experience with 1,279 procedures. Catheter Cardiovasc Diagn 1994;32:332-9.
39. Doorey AJ, Goldenberg EM. Transseptal catheterization in adults: enhanced efficacy and safety by low-volume operators using a "non-standard" technique. Catheter Cardiovasc Diagn 1991;22:239-43.
40. Lundqvist B, Olsson C, Varnauskas SB. Transseptal left heart catheterization: a review of 278 studies. Clin Cardiol 1986;91:21-6.
41. Hurrell DG, Nishimura RA, Symanski JD, Holmes DR Jr. Echocardiography in the invasive laboratory: utility of two-dimensional echocardiography in performing transseptal catheterization. Mayo Clin Proc 1998;73:126-31.
42. Mitchel JF, Gillam LD, Sanzobrino BW, Hirst JA, McKay RG. Intracardiac ultrasound imaging during transseptal catheterization. Chest 1995;108: 104-8.
43. Epstein LM, Smith T, TenHoff H. Nonfluoroscopic transseptal catheterization: safety and efficacy of intracardiac echocardiographic guidance. J Cardiovasc Electrophysiol 1998;9:625-30.
44. Kyo S, Motoyama T, Miyamoto N, Noda H, Dohi Y, Omoto R. Percutaneous introduction of left atrial cannula for left heart bypass: utility of biplane transesophageal echocardiographic guidance for transseptal puncture. Artif Organs 1992;16:386-91.
45. Hanaoka T, Suyama K, Taguchi A, Shimizu W, Kurita T, Aihara N, et al. Shifting of puncture site in the fossa ovalis during radiofrequency catheter ablation: intracardiac echocardiography-guided transseptal left heart catheterization. Jpn Heart J 2003;44:673-80.
46. Hahn K, Gal R, Sarnoski J, Kubota J, Schmidt DH, Bajwa TK. Transesophageal echocardiographically guided atrial transseptal catheterization in patients with normal-sized atria: incidence of complications. Clin Cardiol 1995;18:217-20.
47. Szili-Torok T, Kimman G, Theuns D, Res J, Roelandt JR, Jordaens LJ. Transseptal left heart catheterisation guided by intracardiac echocardiography. Heart 2001;86:11-5.
48. Cafri C, de la Guardia B, Barasch E, Brink J, Smalling RW. Transseptal puncture guided by intracardiac echocardiography during percutaneous transvenous mitral commissurotomy in patients with distorted anatomy of the fossa ovalis. Catheter Cardiovasc Interv 2000;50:463-7.
49. Kronzon I, Glassman E, Cohen M, Winer H. Use of two-dimensional echocardiography during transseptal cardiac catheterization. J Am Coll Cardiol 1984;4:425-8.
50. Hung JS, Fu M, Yeh KH, Chua S, Wu JJ, Chen YC. Usefulness of intracardiac echocardiography in transseptal puncture during percutaneous transvenous mitral commissurotomy. Am J Cardiol 1993;72:853-4.
51. Daoud EG, Kalbfleisch SJ, Hummel JD. Intracardiac echocardiography to guide transseptal left heart catheterization for radiofrequency catheter ablation. J Cardiovasc Electrophysiol 1999;10:358-63.
52. Bishop LHF, Estes EHJ, McIntosh HD. The electrocardiogram as a safeguard in pericardiocentesis. JAMA 1956;162:264-5.
53. Duvernoy O, Borowiec J, Helmius G, Erikson U. Complications of percutaneous pericardiocentesis under fluoroscopic guidance. Acta Radiol 1992;33:309-13.
54. Kerber RE, Ridges JD, Harrison DC. Electrocardiographic indications of atrial puncture during pericardiocentsis. N Engl J Med 1970;282:1142-3.
55. Tsang T, Enriquez-Sarano M, Freeman W, Barnes ME, Sinak LJ, Gersh BJ, et al. Consecutive 1127 therapeutic echocardiographically guided pericardiocenteses: clinical profile, practice patterns, and outcomes spanning 21 years. Mayo Clin Proc 2002;77:429-36.
56. Tsang T, El-Najdawi E, Freeman W, Hagler D, Seward J, O'Leary P. Percutaneous echocardiographically guided pericardiocentesis in pediatric patients: evaluation of safety and efficacy. J Am Soc Echocardiogr 1998;11:1072-7.
57. Tsang T, Freeman W, Barnes M, Reeder G, Packer D, Seward J. Rescue echocardiographically guided pericardiocentesis for cardiac perforation complicating catheter-based procedures: the Mayo Clinic experience. J Am Coll Cardiol 1998;32:1345-50.
58. Tsang T, Barnes M, Hayes S, Freeman WK, Dearani JA, Osborn Butler SL, et al. Clinical and echocardiographic characteristics of significant pericardial effusions following cardiothoracic surgery and outcomes of echo-guided pericardiocentesis for management: Mayo Clinic experience, 1979-1998. Chest 1999;116:322-31.
59. Tsang T, Seward J, Barnes M, Bailey KR, Sinak LJ, Urban LH, et al. Outcomes of primary and secondary treatment of pericardial effusion in patients with malignancy. Mayo Clin Proc 2000;75:248-53.
60. Cauduro S, Moder K, Tsang T, Seward J. Clinical and echocardiographic characteristics of hemodynamically significant pericardial effusions in patients with systemic lupus erythematosus. Am J Cardiol 2003;92:1370-2.
61. Isselbacher EM, Cigarroa JE, Eagle KA. Cardiac tamponade complicating proximal aortic dissection: is pericardiocentesis harmful? Circulation 1994;90:2375-8.
62. Mortensen SA, Egeblad H. Endomyocardial biopsy guided by cross-sectional echocardiography. Br Heart J 1983;50:246-51.
63. Williams GA, Kaintz RP, Habermehl KK, Nelson JG, Kennedy HL. Clinical experience with two-dimensional echocardiography to guide endomyocardial biopsy. Clin Cardiol 1985;8:137-40.
64. Miller LW, Labovitz AJ, McBride LA, Pennington DG, Kanter K. Echocardiography-guided endomyocardial biopsy: a 5-year experience. Circulation 1988;78(suppl):III-99-102.
65. Grande AM, DePieri G, Pederzolli C, Rinaldi M, Vigno M. Echo-guided endomyocardial biopsy in heterotopic heart transplantation: case report. J Cardiovasc Surg 1989;39:223-5.
66. Ragni T, Martivelli L, Goggi C, Speziali G, Rinaldi M, Roda G, et al. Echo-controlled endomyocardial biopsy. J Heart Transplant 1990;9:538-42.
67. Scott BJ, Ettles DF, Rees MR, Williams GJ. The use of combined transesophageal echocardiography and fluoroscopy in the biopsy of a right atrial mass. Br J Radiol 1990;63:222-4.
68. Azuma T, Ohira A, Akagi H, Yamamoto T, Tanaka T. Transvenous biopsy of a right atrial tumor under transesophageal echocardiographic guidance. Am Heart J 1996;131:402-4.
69. Kang SM, Rim SJ, Chang HJ, Choi D, Cho SY, Cho SH, et al. Primary cardiac lymphoma diagnosed by transvenous biopsy under transesophageal echocardiographic guidance and treated with systemic chemotherapy. Echocardiography 2003;20:101-3.
70. Pandian NG, Isner JM, Hougen TJ, Desnoyers MR, McInerney K, Salem DM. Percutaneous balloon valvuloplasty of mitral stenosis aided by cardiac ultrasound. Am J Cardiol 1987;59:380-1.
71. Campbell AN, Hong MK, Pichard AD, Leon MB, Milner MR, Mintz GS, et al. Routine transesophageal echocardiographic guidance is useful during percutaneous transvenous mitral valvuloplasty [abstract]. J Am Soc Echocardiogr 1992;5:330.
72. Kultursay H, Turkogtu C, Akin M, Payzin S, Soydas C, Akilli A. Mitral balloon valvuloplasty with transesophageal echocardiography without using fluoroscopy. Cathet Cardiovasc Diagn 1992;27:317-21.

73. Nigri A, Alessandri N, Martuscelli E, Mangieri E, Berni A, Comito F. Clinical significance of small left-to-right shunts after percutaneous mitral valvuloplasty. Am Heart J 1993;125:783-6.
74. Goldstein SA, Campbell AN. Mitral stenosis: evaluation and guidance of valvuloplasty by transesophageal echocardiography. Cardiol Clin 1993; 11:409-25.
75. Goldstein SA, Campbell A, Mintz GS, Pichard A, Leon M, Lindsay J Jr. Feasibility of on-line transesophageal echocardiography during balloon mitral valvulotomy: experience with 93 patients. J Heart Valve Dis 1994;3:136-48.
76. Wilkins GT, Weyman AE, Abascal VM, Block P, Palacios IF. Percutaneous balloon dilatation of the mitral valve: an analysis of echocardiographic variables related to outcome and the mechanism of dilatation. Br Heart J 1998;60:299-308.
77. Reid CL, Chandraratna AN, Kawanishi DT, Kotlewski A, Rahimtoola SH. Influence of mitral valve morphology on double-balloon valvuloplasty in patients with mitral stenosis: analysis of factors predicting immediate and 3-month results. Circulation 1989;80:515-24.
78. Green NE, Hansgen AR, Carroll JD. Initial clinical experience with intracardiac echocardiography in guiding balloon mitral valvuloplasty: technique, safety, utility, and limitations. Catheter Cardiovasc Interv 2004; 63:385-94.
79. Srinivasa KH, Manjunath CN, Dhanalakshmi C, Patil C, Venkatesh HV. Transesophageal Doppler echocardiographic study of pulmonary venous flow pattern in severe mitral stenosis and the changes following balloon mitral valvuloplasty. Echocardiography 2000;17:151-7.
80. Inoue K, Owaki T, Nakamura T, Kitamura F, Miyamoto N. Clinical applications of transvenous mitral commissurotomy by a new balloon catheter. J Thorac Cardiovasc Surg 1984;87:394-402.
81. Kandpal B, Gary N, Anand KV, Kapoor A, Sinha N. Role of oral anticoagulation and Inoue balloon mitral valvulotomy in presence of left atrial thrombus: a prospective serial transesophageal echocardiographic study. J Heart Valve Dis 2002;11:594-600.
82. Waksmonski CA, McKay RG. Echocardiographic diagnosis of valve disruption following percutaneous balloon valvuloplasty. Echocardiography 1989;6:277-81.
83. Park S-H, Kim M-A, Hyon M-S. The advantages of on-line transesophageal echocardiography guide during percutaneous balloon mitral valvuloplasty. J Am Soc Echocardiogr 2000;13:26-34.
84. Chiang C-W, Hsu L-A, Chu P-H, Ko Y-S, Ko Y-L, Cheng NJ, et al. On-line multiplane transesophageal echocardiography for balloon mitral commissurotomy. Am J Cardiol 1998;81:515-8.
85. Applebaum RM, Kasliwal RR, Kanojia A, Seth A, Bhandari S, Trehan N, et al. Utility of three-dimensional echocardiography during balloon mitral valvuloplasty. J Am Coll Cardiol 1998;32:1405-9.
86. Iung B, Cormier B, Discimetiere P, Porte J-M, Nallet O, Michel P-L, et al. Functional results 5 years after successful percutaneous mitral commissurotomy in a series of 508 patients and analysis of predictive factors. J Am Coll Cardiol 1996;27:407-14.
87. Yeh KH, Kung JS, Wu CJ, Fu M, Chua S, Chern M. Safety of Inoue balloon mitral commissurotomy in patients with left atrial appendage thrombi. Am J Cardiol 1995;75:302-4.
88. Earing MG, Cabalka AK, Seward JB, Bruce CJ, Reeder GS, Hagler DJ. Intracardiac echocardiographic guidance during transcatheter device closure of atrial septal defect and patent foramen ovale. Mayo Clin Proc 2004;79:24-34.
89. Lopez L, Ventura R, Welch EM, Nykanen DG, Zahn EM. Echocardiographic considerations during deployment of the Helex septal occluder for closure of atrial septal defects. Cardiol Young 2003;13:290-8.
90. Du ZD, Koenig P, Cao QL, Waight D, Heitschmidt M, Hijazi ZM. Comparison of transcatheter closure of secundum atrial septal defect using the Amplatzer septal occluder associated with deficient versus sufficient rims. Am J Cardiol 2002;90:865-9.
91. Alboliras ET, Hijazi ZM. Comparison of costs of intracardiac echocardiography and transesophageal echocardiography in monitoring percutaneous device closure of atrial septal defect in children and adults. Am J Cardiol 2004;94:690-2.
92. Momenah TS, McElhinney DB, Brook MM, Moore P, Silverman NH. Transesophageal echocardiographic predictors for successful transcatheter closure of defects within the oval fossa using the CardioSEAL septal occlusion device. Cardiol Young 2000;10:510-8.
93. Nishimura RA, Holmes DR. Hypertrophic cardiomyopathy. N Engl J Med 2004;350:1320-7.
94. Maron BJ, Dearani JA, Ommen SR, Maron MS, Schaff HV, Gersh BJ, et al. The case for surgery in obstructive hypertrophic cardiomyopathy. J Am Coll Cardiol 2004;44:2044-53.
95. Fananapazir L, Epstein ND, Curiel RV, Panza JA, Tripodi D, McAreavery D. Long-term results of dual-chamber (DDD) pacing in obstructive hypertrophic cardiomyopathy: evidence for progressive symptomatic and hemodynamic improvement and reduction of left ventricular hypertrophy. Circulation 1994;90:2731-42.
96. Sigwart U. Non-surgical myocardial reduction for hypertrophic obstructive cardiomyopathy. Lancet 1995;346:211-4.
97. Seggewiss H, Gleichmann U, Faber L, Fassbender D, Schmidt HK, Strick S. Percutaneous transluminal septal myocardial ablation in hypertrophic obstructive cardiomyopathy: acute results and 3-month follow-up in 25 patients. J Am Coll Cardiol 1998;31:252-8.
98. Lakkis NM, Nagueh SF, Kleiman NS, Killip D, He Z-X, Verani MS, et al. Echocardiography-guided ethanol septal reduction for hypertrophic obstructive cardiomyopathy. Circulation 1998;98:1750-5.
99. Kimmelstiel CD, Maron BJ. Role of percutaneous septal ablation in hypertrophic obstructive cardiomyopathy. Circulation 2004;109:452-5.
100. Faber L, Seggewiss H, Welge D, Fassbender D, Schmidt HK, Gleichmann U, et al. Echo-guided percutaneous septal ablation for symptomatic hypertrophic cardiomyopathy: 7 years of experience. Eur J Echocardiogr 2004;5: 347-55.
101. Hess OM, Sigwart U. New treatment strategies for hypertrophic obstructive cardiomyopathy: alcohol ablation of the septum: the new gold standard? J Am Coll Cardiol 2004;44:2054-5.
102. Faber L, Seggewiss H, Gleichmann U. Percutaneous transluminal septal myocardial ablation in hypertrophic obstructive cardiomyopathy: results with respect to intra-procedural myocardial contrast echocardiography. Circulation 1998;98:2415-21.
103. Kuhn H, Gietzen FH, Schafers M, Freick M, Gockel B, Strunk-Muller C, et al. Changes in the left ventricular outflow tract after transcoronary ablation of septal hypertrophy (TASH) for hypertrophic obstructive cardiomyopathy as assessed by transesophageal echocardiography and by measuring myocardial glucose utilization and perfusion. Eur Heart J 1999;20:1808-17.
104. Faber L, Meissner A, Ziemssen P, Seggewiss H. Percutaneous transluminal septal myocardial ablation for hypertrophic cardiomyopathy. Heart 2000;83:326-31.
105. Faber L, Ziemssen P, Seggewiss H. Targeting percutaneous transluminal septal ablation for hypertrophic obstructive cardiomyopathy by intraprocedural echocardiographic monitoring. J Am Soc Echocardiogr 2000;13: 1074-9.
106. Flores-Ramirez R, Lakkis NM, Middleton KJ, Killip D, Spencer WH III, Nagueh SF. Echocardiographic insights into the mechanisms of relief of left ventricular outflow tract obstruction after nonsurgical septal reduction therapy in patients with hypertrophic obstructive cardiomyopathy. J Am Coll Cardiol 2001;37:208-14.
107. Nagueh SF, Lakkis NM, He ZX, Middleton KJ, Killip D, Zoghbi WA, et al. Role of myocardial contrast echocardiography during non-surgical septal reduction therapy for hypertrophic obstructive cardiomyopathy. J Am Coll Cardiol 1998;32:225-9.
108. Maron BJ, McKenna WJ, Danielson GK, Kappenberger LJ, Kuhn HJ, Seidman CE, et al., for the Task Force on Clinical Expert Consensus Documents, American College of Cardiology, and Committee for Practice Guidelines, European Society of Cardiology. American College of Cardiology/European Society of Cardiology clinical expert consensus document on hypertrophic cardiomyopathy: a report of the American College of Cardiology Foundation Task Force on Clinical Expert Consensus Documents and the European Society of Cardiology Committee for Practice Guidelines. J Am Coll Cardiol 2003;42:1687-713.

109. Maron BJ, McKenna WJ, Danielson GK, Kappenberger LJ, Kuhn HJ, Seidman CE, et al, for the American College of Cardiology Foundation Task Force on Clinical Expert Consensus Documents, and European Society of Cardiology, Committee for Practice Guidelines. American College of Cardiology/European Society of Cardiology clinical expert consensus document on hypertrophic cardiomyopathy: a report of the American College of Cardiology Foundation Task Force on Clinical Expert Consensus Documents and the European Society of Cardiology Committee for Practice Guidelines. Eur Heart J 2003;24:1965-91.
110. Olgin JE, Kalman JM, Fitzpatrick AP, Lesh MD. Role of right atrial endocardial structures as barriers to conduction during human type I atrial flutter: activation and entrainment mapping guided by intracardiac echocardiography. Circulation 1995;92:1839-48.
111. Kalman JM, Olgin JE, Saxon LA, Fisher WG, Lee RJ, Lesh MD. Activation and entrainment mapping defines the tricuspid annulus as the anterior barrier in typical atrial flutter. Circulation 1996;94:398-406.
112. Saxon LA, Stevenson WG, Fonarow GC, Middlekauff HR, Yeatman LA, Sherman CT, et al. Transesophageal echocardiography during radiofrequency catheter ablation of ventricular tachycardia. Am J Cardiol 1993;72:658-61.
113. Packer D, Kapler J, Hammill S, Stanton M, Khandheria B, Seward J. Characterization of the pathophysiologic sequelae of the impedance rise during radiofrequency ablation of accessory pathways. Circulation 1991;84: II-709.
114. Goldman AP, Irwin JM, Glover MU, Mick W. Transesophageal echocardiography to improve positioning of radiofrequency ablation catheters in left-sided Wolff-Parkinson-White syndrome. Pacing Clin Electrophysiol 1991;14:1245-50.
115. Lai WW, Al-Khatib Y, Klitzner TS, Child JS, Wetzel GT, Saxon LA, et al. Biplanar transesophageal echocardiographic direction of radiofrequency catheter ablation in children and adolescents with the Wolff-Parkinson-White syndrome. Am J Cardiol 1993;71:872-4.
116. Packer DL, Stevens CL, Curley MG, Bruce CJ, Miller FA, Khandheria BK, et al. Intracardiac phased-array imaging methods and initial clinical experience with high resolution, under blood visualization: initial experience with intracardiac phased-array ultrasound. J Am Coll Cardiol 2002;39: 509-16.
117. Olgin JE, Kalman JM, Chin M, Stillson C, Maguire M, Ursel P, et al. Electrophysiological effects of long, linear atrial lesions placed under intracardiac ultrasound guidance. Circulation 1997;96:2715-21.
118. Epstein LM, Mitchell MA, Smith TW, Haines DE. Comparative study of fluoroscopy and intracardiac echocardiographic guidance for the creation of linear atrial lesions. Circulation 1998;98:1796-801.
119. Roithinger FX, Steiner PR, Godeki Y, Goseki Y, Liese KS, Scholtz DB, et al. Low-power radiofrequency application and intracardiac echocardiography for creation of continuous left atrial linear lesions. J Cardiovasc Electrophysiol 1999;10:680-91.
120. Chugh SS, Chan RC, Johnson SB, Packer DL. Catheter tip orientation affects radiofrequency ablation lesion size in the canine left ventricle. Pacing Clin Electrophysiol 1999;22:413-20.
121. Chan RC, Johnson SB, Seward JB, Packer DL. The effect of ablation electrode length and catheter tip/endocardial orientation on radiofrequency lesion size in the canine right atrium. Pacing Clin Electrophysiol 2002;25: 4-13.
122. Doi A, Takagi M, Toda I, Teragaki M, Yoshiyama M, Takeuchi K, et al. Real time quantification of low temperature radiofrequency ablation lesion size using phased array intracardiac echocardiography in the canine model: comparison of two-dimensional images with pathological lesion characteristics. Heart 2003;89:923-7.
123. Roman-Gonzalez J, Johnson SB, Wahl MR, Packer DL. Utility of echocontrast for accurate prediction of chronic radiofrequency lesion dimensions in ventricular tissue. Pacing Clin Electrophysiol 2001;24: 681A.
124. Kalman JM, Olgin JE, Karch MR, Hamdan M, Lee RJ, Lesh MD. "Cristal tachycardias": origin of right atrial tachycardias from the crista terminalis identified by intracardiac echocardiography. J Am Coll Cardiol 1998;31: 451-9.
125. Batra R, Nair M, Kumar M, Mohan J, Shah P, Kaul U, et al. Intracardiac echocardiography guided radiofrequency catheter ablation of the slow pathway in atrioventricular nodal reentrant tachycardia. J Interv Card Electrophysiol 2002;6:43-9.
126. Kalman JLR, Fisher WG, Chin MC, Fisher WG, Chin MC, Ursell P, et al. Radiofrequency catheter modification of sinus pacemaker function guided by intracardiac echocardiography. Circulation 1995;92:3070-81.
127. Jongbloed MR, Bax JJ, Zeppenfeld K, van der Wall EE, Schalij MJ. Anatomical observations of the pulmonary veins with intracardiac echocardiography and hemodynamic consequences of narrowing of pulmonary vein ostial diameters after radiofrequency catheter ablation of atrial fibrillation. Am J Cardiol 2004;93:1298-302.
128. Okishige K, Kawabata M, Yamashiro K, Ohshiro C, Umayahara S, Gotoh M, et al. Clinical study regarding the anatomical structures of the right atrial isthmus using intra-cardiac echocardiography: implication for catheter ablation of common atrial flutter. J Interv Card Electrophysiol 2005;12:9-12.
129. Morton JB, Sanders P, Davidson NC, Sparks PB, Vohra JK, Kalman JM. Phased-array intracardiac echocardiography for defining cavotricuspid isthmus anatomy during radiofrequency ablation of typical atrial flutter. J Cardiovasc Electrophysiol 2003;14:591-7.
130. Packer DL, Monahan KH, Peterson LA, Friedman PA, Munger TM, Hammill SC, et al. Predictors of successful atrial fibrillation ablation through pulmonary vein isolation. Pacing Clin Electrophysiol 2003;26: 962.
131. Razavi M, Munger TM, Shen WK, Packer DL. Intracardiac ultrasound validation of dense scar delineation by electro-anatomic voltage mapping. Pacing Clin Electrophysiol 2003;26:930.
132. Callans DJ, Ren JF, Narula N, Michele J, Marchlinski FE, Dillon SM. Effects of linear, irrigated-tip radiofrequency ablation in porcine healed anterior infarction. J Cardiovasc Electrophysiol 2001;12:1037-42.
133. Wilber DJ, Kopp DE, Glascock DN, Kinder CA, Kall JG. Catheter ablation of the mitral isthmus for ventricular tachycardia associated with inferior infarction. Circulation 1995;92:3481-9.
134. Arruda M, Wang ZT, Patel A, Anders RA, Kall JG, Kopp D, et al. Intracardiac echocardiography identifies pulmonary vein ostea more accurately than conventional angiography. J Am Coll Cardiol 2000;35:110A.
135. Wood MA, Wittkamp M, Henry D, Martin R, Nixon JV, Shepard RK, et al. A Comparison of pulmonary vein ostial anatomy by computerized tomography, echocardiography, and venography in patients with atrial fibrillation having radiofrequency catheter ablation. Am J Cardiol 2004; 93:49-53.
136. Asirvatham S, Friedman PA, Packer DL, Edwards WD. Is there an endocardial marker for the vein/ligament of Marshall? Circulation 2001;104: II-568.
137. Packer DL, Darbar D, Bluhm CM, Monahan KH, Peterson L, Munger TM, et al. Utility of phased-array intracardiac ultrasound for guiding the positioning of the lasso mapping catheter in pulmonary veins undergoing AF ablation [abstract]. Circulation 2001;104:II-620.
138. Swarup V, Azegami K, Arruda M, Burke MC, Lin AC, Wilber DJ. Four-vessel pulmonary vein isolation guided by intra-cardiac echocardiography without contrast venography in patients with drug refractory paroxysmal atrial fibrillation [abstract]. J Am Coll Cardiol 2002; 39:114A.
139. Bunch TJ, Bruce GK, Johnson SB, Milton MA, Sarabanda AV, Packer DL. Analysis of catheter-tip (8-mm) and actual tissue temperatures achieved during radiofrequency ablation at the orifice of the pulmonary vein. Circulation 2004;110:2988-95.
140. Verma A, Marrouche NF, Natale A. Pulmonary vein antrum isolation: intracardiac echocardiography-guided technique. J Cardiovasc Electrophysiol 2004;15:1335-40.
141. Bruce GK, Milton MA, Bunch TJ, Sarabanda A, Johnson SB, Packer DL. Catheter tip/tissue temperature discrepancies in cooled-tip ablation: relevance to guiding left atrial ablation. Circulation 2005;12:954-60.
142. Asirvatham S, Packer DL, Johnson SB. Ultrasound vs. temperature feedback monitoring microcatheter ablation in the canine atrium [abstract]. Pacing Clin Electrophysiol 1999;22:822A.

143. Roman-Gonzalez J, Asirvatham S, Razavi M, Packer DL, Grice SK, Friedman PA, et al. Marked discrepancies between catheter tip temperature registration and pulmonary vein tissue changes during ablation of focal atrial fibrillation in patients [abstract]. Pacing Clin Electrophysiol 2001;24:656A.
144. Ren JF, Marchlinski FE, Callans SJ. Left atrial thrombus associated with ablation for atrial fibrillation: identification with intracardiac echocardiography. J Am Coll Cardiol 2004;43:1861-7.
145. Bruce CJ, Friedman PA, Asirvatham SJ, Munger TM, Shen W-K, Peterson LA, et al. Frequency of left atrial thrombus occurrence in patients with atrial fibrillation during pulmonary vein isolation despite anticoagulation [abstract]. Circulation 2003;108:IV-321.
146. Ren JF, Marchlinski FE, Callans DJ, Zado ES. Intracardiac Doppler echocardiographic quantification of pulmonary vein flow velocity: an effective technique for monitoring pulmonary vein ostia narrowing during focal atrial fibrillation ablation. J Cardiovasc Electrophysiol 2002;13:1076-81.
147. Saad EB, Cole CR, Marrouche NF, Dresing TJ, Perez-Lugones A, Saliba WI, et al. Use of intracardiac echocardiography for prediction of chronic pulmonary vein stenosis after ablation of atrial fibrillation. J Cardiovasc Electrophysiol 2002;13:986-9.
148. Ren JF, Marchlinski FE, Callans DJ. Effect of heart rate and isoproterenol on pulmonary vein flow velocity following radiofrequency ablation: a Doppler color flow imaging study. J Interv Card Electrophysiol 2004; 10:265-9.
149. Alfieri O, De Bonis M, Lapenna E, Regesta T, Maisano F, Torracca L, et al. "Edge-to-edge" repair for anterior mitral leaflet prolapse. Semin Thorac Cardiovasc Surg 2004;16:182-7.
150. De Bonis M, Lapenna E, La Canna G, Ficarra E, Pagliaro M, Torracca L, et al. Mitral valve repair for functional mitral regurgitation in end-stage dilated cardiomyopathy: role of the "edge-to-edge" technique. Circulation 2005;112:I-402-8.
151. Maisano F, Torracca L, Oppizzi M, Stefano PL, D'Addario G, LaCanna G, et al. The edge-to-edge technique: a simplified method to correct mitral insufficiency. Eur J Cardiothorac Surg 1998;13:240-5.
152. Alfieri O, Maisano F, Colombo A, Pappone C, La Canna G, Zangrillo A. Percutaneous mitral valve repair: an attractive perspective and an opportunity for teamwork. Ital Heart J 2004;5:723-6.
153. Block PC. Percutaneous mitral valve repair for mitral regurgitation. J Intervent Cardiol 2003;16:93-6.
154. Daimon M, Shiota T, Gillinov AM, Hayase M, Ruel M, Cohn WE, et al. Percutaneous mitral valve repair for chronic ischemic mitral regurgitation: a real-time three-dimensional echocardiographic study in an ovine model. Circulation 2005;111:2183-9.
155. Feldman T, Wasserman HS, Herrmann HC, Gray W, Block PC, Whitlow P, et al. Percutaneous mitral valve repair using the edge-to-edge technique: six-month results of the EVEREST phase I clinical trial. J Am Coll Cardiol 2005;46:2134-40.
156. Herrmann HC, Wasserman HS, Whitlow P, Block PC, Gray WA, Foster E, et al. Percutaneous edge-to-edge mitral valve repair using the Evalve MitraClip™ device: initial one year results of the EVEREST phase 1 trial [abstract]. Circulation 2005;112:II-520.
157. Liddicoat JR, MacNeill BD, Gillinov AM, Cohn WE, Chin C-H, Prado AD, et al. Percutaneous mitral valve repair: a feasibility study in an ovine model of acute ischemic mitral regurgitation. Catheter Cardiovasc Interv 2003;60:410-6.
158. Palacios IF. Percutaneous valve replacement and repair: fiction or reality? J Am Coll Cardiol 2004;44:1662-3.
159. Madden J. Resection of the left auricular appendix. JAMA 1948;140: 769-72.
160. Bailey C, Olsen A, Keown K, Nichols HT, Jamison WL. Commissurotomy for mitral stenosis technique for prevention of cerebral complications. JAMA 1952;149:1085-91.
161. Belcher JR, Somerville W. Systemic embolism and left atrial thrombosis in relation to mitral stenosis. Br Med J 1955;2:1000-3.
162. Bonow RO, Carabello B, de Leon AC Jr, Edmunds LH Jr, Fedderly BJ, Freed MD, et al. ACC/AHA guidelines for the management of patients with valvular heart disease: a report of the American College of Cardiology/American Heart Association Task Force on Practice Guidelines (Committee on Management of Patients With Valvular Heart Disease). J Am Coll Cardiol 1998;32:1486-582.
163. Cox JL. The surgical treatment of atrial fibrillation, IV: surgical technique. J Thorac Cardiovasc Surg 1991;101:584-92.
164. Johnson WD, Ganjoo AK, Stone CD, Srivyas RC, Howard M. The left atrial appendage: our most lethal human attachment: surgical implications. Eur J Cardiothorac Surg 2000;17:718-22.
165. Sievert H, Lesh MD, Trepels T, Omran H, Bartorelli A, Bella PD, et al. Percutaneous left atrial appendage transcatheter occlusion to prevent stroke in high-risk patients with atrial fibrillation. Circulation 2002; 105:1887-9.
166. Hanna IR, Kolm P, Martin R, Reisman M, Gray W, Block PC. Left atrial structure and function after percutaneous left atrial appendage transcatheter occlusion (PLAATO): six-month echocardiographic follow-up. J Am Coll Cardiol 2004;43:1868-72.
167. Sick PB, Schuler G, Hauptmann KE, Grube E, Yakubov S, Turi ZG, et al. Initial Worldwide experience with the WATCHMAN left atrial appendage system for stroke prevention in atrial fibrillation. J Am Coll Cardiol 2007;49:1490-5.
168. McCreery CJ, McCulloch M, Ahmad M, deFilippi CR. Real-time 3-dimensional echocardiography imaging for right ventricular endomyocardial biopsy: a comparison with fluoroscopy. J Am Soc Echocardiogr 2001;14:927-33.
169. Chauvel C, Bogino E, Clerc P, Fernandez G, Vernhet J-C, Becat A, et al. Usefulness of three-dimensional echocardiography for the evaluation of mitral valve prolapse: an intraoperative study. J Heart Valve Dis 2000;9:341-9.
170. Sutaria N, Northridge D, Masani N, Pandian N. Three dimensional echocardiography for the assessment of mitral valve disease. Heart 2000;84: 7-10.
171. Ahmed S, Nanda NC, Miller AP, Nekkanti R, Yousif AM, Pacifico AD, et al. Usefulness of transesophageal three-dimensional echocardiography in the identification of individual segment/scallop prolapse of the mitral valve. Echocardiography 2003;20:203-9.
172. Langerveld J, Valocik G, Plokker HWT, Ernst SMPG, Mannaerts FJ, Kelder JC, et al. Additional value of three-dimensional transesophageal echocardiography for patients with mitral valve stenosis undergoing balloon valvuloplasty. J Am Soc Echocardiogr 2003;16:841-9.
173. Sugeng L, Weinert L, Lammertin G, Thomas P, Spencer KT, DeCara JM, et al. Accuracy of mitral valve area measurements using transthoracic rapid freehand 3-dimensional scanning: comparison with noninvasive and invasive methods. J Am Soc Echocardiogr 2003;16:1292-300.
174. Fann JI, St Goar FG, Komtebedde J, Oz MC, Block PC, Foster E, et al. Beating heart catheter-based edge-to-edge mitral valve procedure in a porcine model: efficacy and healing response. Circulation 2004;110: 988-93.
175. Cooke JC, Gelman JS, Harper RW. Echocardiologists' role in the deployment of the Amplatzer atrial septal occluder device in adults. J Am Soc Echocardiogr 2001;14:588-94.
176. Maeno Y, Benson L, Boutin C. Impact of dynamic 3D transesophageal echocardiography in the assessment of atrial septal defects and occlusion by the double-umbrella device (CardioSEAL). Cardiol Young 1998;8:368-78.
177. Sinha A, Nanda NC, Misra V, Khanna D, Dod HS, Vengala S, et al. Live three-dimensional transthoracic echocardiographic assessment of transcatheter closure of atrial septal defect and patent foramen ovale. Echocardiography 2004;21:749-53.
178. Cribier A, Eltchaninoff H, Bash A, Borenstein N, Tron C, Bauer F, et al. Percutaneous transcatheter implantation of an aortic valve prosthesis for calcific aortic stenosis: first human case description. Circulation 2002;106:3006-8.
179. Cribier A, Eltchaninoff H, Tron C, Bauer F, Agatiello C, Sebagh L, et al. Early experience with percutaneous transcatheter implantation of heart valve prosthesis for the treatment of end-stage inoperable patients with calcific aortic stenosis. J Am Coll Cardiol 2004;43:698-703.
180. Lichtenstein SV, Cheung A, Ye J, Thompson CR, Carere RG, Pasupati S, et al. Transapical transcatheter aortic valve implantation in humans: initial clinical experience. Circulation 2006;114:591-6.

181. Webb JG, Pasupati S, Humphries K, Thompson C, Altwegg L, Moss R, et al. Percutaneous transarterial aortic valve replacement in selected high-risk patients with aortic stenosis. Circulation 2007;116:755-63.
182. Ye J, Cheung A, Lichtenstein SV, Pasupati S, Carere RG, Thompson CR, et al. Six-month outcome of transapical transcatheter aortic valve implantation in the initial seven patients. Eur J Cardiothorac Surg 2007;31: 16-21.
183. Moss RG, Ivens E, Pasupati S, Humphries K, Thompson C, Munt B. Role of echocardiography in percutaneous aortic valve implantation. J Am Coll Cardiol Imaging 2008;1:15-24.
184. Berry C, Oukerrag L, Asgar A, Lamarche Y, Marcheix B, Denault AY, et al. Role of transesophageal echocardiography in percutaneous aortic valve replacement with the CoreValve revalving system. Echocardiography 2008;25:840-8.